FabF and FadM Cooperate to Recycle Fatty Acids and Rescue Δ*plsX* Lethality in *Staphylococcus aureus*

Paprapach Wongdontree[1], Milya Palmier[1], Clara Louche[1], Vincent Leguillier[1], Carine Machado Rodrigues[2], Karine Gloux[1], David Halpern[1], Céline Henry[2], Jamila Anba-Mondoloni[1], Alexandra Gruss[1#]

[1] Université Paris-Saclay, INRAE, AgroParisTech, Micalis Institute, 78350, Jouy-en-Josas, France.

[#] For correspondence: alexandra.gruss@inrae.fr

Keywords: *Staphylococcus aureus,* MRSA, fatty acid, FASII, phospholipid synthesis, *plsX* deletion suppressors, FabF, platensimycin, FadM, acyl-CoA thioesterase, acyl-ACP thioesterase, ACP binding, membrane, β-lactam sensitivity.

Short title: FabF-FadM role in fatty acid recycling

Abstract

Phospholipids are essential components of most cell membranes. In *Staphylococcus aureus*, PlsX acyltransferase is considered indispensable for initiating phospholipid synthesis, unless exogenous fatty acids (FAs) are available to bypass this requirement. We report that *S. aureus* can capture internal FA sources to overcome PlsX essentiality in a Δ*plsX* mutant *via* point mutations in either of two genes: *fabF*, which encodes the FA synthesis enzyme 3-oxoacyl-(acyl-carrier-protein) synthase II, or *fadM*, which encodes an understudied bifunctional acyl-CoA thioesterase and ACP binding protein. Despite growth rescue, both Δ*plsX* suppressors differ from the parental strain by producing phospholipids with shortened FA lengths suggesting that both suppressors lead to premature FA release during synthesis. Additionally, both suppressors display increased sensitivity to β-lactam antibiotics. The similar behavior of both suppressors led us to show that *fabF* suppressors require the presence of *fadM*, indicative of FabF-FadM cooperation. We propose that reduced processivity of FabF suppressor variants, or greater availability of FadM for ACP binding in FadM variants, facilitates FA release from FabF-acyl-ACP intermediates. A FabF-FadM relay leading to FA release may contribute to homeostasis between FASII and phospholipid synthesis pathways.

Significance

Phospholipids are vital cell membrane components. The essential *Staphylococcus aureus* phospholipid synthesis enzyme PlsX uses acyl-ACP, the end-product of fatty acid (FA) synthesis (FASII), to initiate phospholipid production. Despite its central role, PlsX can be substituted by exogenous FAs whose phosphorylation yields the same product. We discovered that without FA supplementation, mutants arise that rescue growth, indicating that internal FAs are released. Mutations occurred in either FabF, a FASII enzyme, or in FadM, an incompletely characterized protein. Our analyses give evidence that FabF and FadM proteins cooperate, and facilitate FA availability when either protein is mutated. We propose that in normal conditions, FadM might act as an “overflow valve” by releasing FAs from the FabF intermediate, which prevents buildup of FASII intermediates, and ensures FA-phospholipid balance. Remarkably, while this pathway rescues *S. aureus* growth, it sensitizes the MRSA strain to β-lactam antibiotics.

63 **Introduction**

64

65 Lipids provide the essential scaffolding for cell membranes and life. Bacterial phospholipid
66 membranes comprise fatty acids (FA) that are attached to a glycerophosphate backbone [1].
67 The phospholipid FAs are either produced by the FA synthesis (FASII) pathway or captured
68 from the environment [2]. The FASII product, acyl-Acyl Carrier Protein (acyl-ACP or FA-ACP)
69 is a substrate for three enzymes: FabF for FA elongation *via* FASII, and PlsX and PlsC for
70 respectively the first and second steps of phospholipid synthesis (**Fig. 1**).

71 The membrane-associated acyltransferase PlsX catalyzes the first dedicated step of
72 phospholipid synthesis in Bacillota bacteria, by reversibly catalyzing conversion of acyl-ACP,
73 the FASII product, to acyl-phosphate (acyl-PO_4) [3]. An alternative phospholipid initiation
74 mechanism, not requiring PlsX, involves assimilation of exogenous FAs *via* phosphorylation
75 by the FA kinase Fak [4]. The membrane glycerol-3-phosphate acyltransferase PlsY then
76 transfers the FA moiety of acyl-PO_4 to the 1-position of the glycerophosphate backbone,
77 forming lysophosphatidic acid. However, reverse PlsX activity may also reconvert acyl-PO_4 to
78 acyl-ACP when exogenous FAs are available, which then re-enter the FASII system or are used
79 by PlsC for phospholipid synthesis [4, 5] (**Fig. 1**). Providing acyl-ACP by PlsX reverse activity
80 on exogenous FAs, once phosphorylated, allows bacteria to overcome the need for FASII,
81 making them insensitive to FASII inhibitors [6-8]. In *Bacillus subtilis*, PlsX is membrane-
82 associated for phospholipid synthesis, which could facilitate acyl-PO_4 transfer to PlsY, but
83 likely not for its reverse activity [9]. PlsX is thus a sorting station that initiates phospholipid
84 synthesis, or returns acyl groups for FASII elongation and PlsC processing.

85 When exogenous FAs are absent, PlsX may still be dispensable in some bacteria.
86 Numerous Pseudomonadota bacteria encode PlsB, which has functional redundancy to PlsX-
87 PlsY [3]. In *E. coli*, suppressors of the synthetic lethal Δ*plsX* Δ*plsY* mutation (despite the
88 existence of the functionally redundant enzyme PlsB [3]) [10] displayed increased pools of
89 glycerol-3-phosphate (Gly-3-P), the backbone for FA attachment to produce phospholipids
90 [10]. Increased Gly-3-P was suggested to compensate the low efficiency acyl-transferase
91 activity of PlsB compared to PlsY. Among Bacillota pathogens, some deploy an acyl-ACP
92 thioesterase (acyl-ACP TE) that liberates endogenous FAs from acyl-ACP**,** which are then
93 phosphorylated by Fak to initiate phospholipid synthesis [11-14]. Acyl-ACP TE fully restores
94 growth of *Streptococcus pneumoniae* Δ*plsX* [12], and conditionally rescues *Enterococcus*
95 *faecalis* Δ*plsX* growth; however, the acyl-ACP TE preferentially cleaves acyl-ACP comprising

96 unsaturated FAs, while growth is stimulated by saturated FAs [13]. These alternative systems
97 in Bacillota all generate an internal FA supply to initiate phospholipid synthesis when PlsX
98 function is impaired.

99 The major human pathogen *Staphylococcus aureus* lacks PlsB, and an acyl-ACP TE to
100 liberate FAs, and only exogenous FAs or a cloned gene encoding heterologous acyl-ACP TE
101 reportedly complemented growth of a *plsX* deletion strain [5]. Our previous work on FASII
102 bypass revealed that exogenous FAs rescue *S. aureus* growth by one of two processes: point
103 mutations that disable *fabD* [7], or by non-mutational adaptation in which FAs are efficiently
104 incorporated after a 6-8 h time lag [6-8]. These studies led us to now investigate the step
105 following FASII, mediated by PlsX. For this we constructed Δ*plsX* mutants, and unexpectedly
106 identified suppressors conferring growth. In this report, we characterized activity-altering
107 mutations mapping to two distinct loci that rescue Δ*plsX* viability without exogenous FAs.
108 Mutations in FASII enzyme FabF, a 3-oxoacyl-ACP synthase II, or in an incompletely
109 characterized acyl-CoA thioesterase and ACP binding protein designated as FadM, rescue
110 Δ*plsX* growth. Our findings reveal that *plsX* essentiality is abolished by point mutations in
111 *fabF* or *fadM*. We demonstrate interdependency of FabF and FadM in rescuing the absence
112 of PlsX. These findings may indicate a general role for FadM as a newly found actor shuttling
113 FAs from FASII towards phospholipid synthesis. Remarkably, the *fabF* and *fadM* suppressors
114 rescue Δ*plsX* growth, but sensitize an MRSA *S. aureus* strain to the β-lactam antibiotic
115 amoxicillin.
116
117
118 **Results**
119
120 **Construction and confirmation of a Δ*plsX* in-frame mutant.** *plsX* is the second gene in a
121 multicistronic operon also comprising FASII genes (**Supplementary Fig. S1**). We constructed
122 in-frame Δ*plsX* mutants of RN-R (RN4220 repaired for a defective *fakB1* gene in the 8325
123 lineage [15]) and of USA300_FPR3757 JE2 strains. Both Δ*plsX* mutants failed to grow on BHI
124 solid medium in the absence of FAs. Deletions were confirmed by PCR and whole genome
125 sequencing (**Table S1**) and by RN-R Δ*plsX* growth complementation in the absence of FAs
126 using a plasmid-carried copy of the intact *plsX* gene (**Supplementary Fig. S2**).
127
128 **FA auxotrophy of *S. aureus* Δ*plsX* mutants is suppressed by a point mutation in *fabF*.** During
129 phenotypic characterization of the JE2 Δ*plsX* mutant, we noted the appearance of colonies

130 on BHI medium without added FA (**Fig. 2A**, left plate). Note that BHI reportedly contains
131 traces of FA [16], but which are insufficient to confer Δ*plsX* growth. Two colonies subjected
132 to whole genome sequencing confirmed the in-frame *plsX* deletion and also revealed point
133 mutations mapping to FabF (SAUSA300_0886), the 3-oxoacyl-ACP synthase II of the FASII
134 elongation cycle (see **Fig. 1**), producing $FabF^{A119E}$ (alanine to glutamic acid; Sup1) and
135 $FabF^{D266A}$ (aspartic acid to alanine; Sup2). The suppressor carrying $FabF^{D266A}$ was not
136 recoverable from the primary stocked strain, possibly because the mutation was deleterious
137 for growth. Sup1 and Sup2 also carried the same point mutation in *csa1A* (SAUSA300_0100),
138 encoding a tandem lipoprotein.

139 We expanded our analyses by isolating 31 other Δ*plsX* suppressors from RN-R or JE2
140 backgrounds (16 and 15 suppressors, respectively), and screened for those carrying *fabF*
141 mutations by PCR followed by DNA sequence analyses (**Table S2**). Among them, 14 carried
142 *fabF* mutations, which mapped to the same *fabF* nucleotide position in both strain
143 backgrounds, resulting in a $FabF^{A119E}$ alteration as in Sup1. This allele is referred to as *fabF1*.
144 *csa1A*, which carried a mutation in Sup1 and Sup2 mutants, was not mutated in the 14 *fabF*
145 mutants, indicating that *fabF* was the suppressor allele. Emergence of the same *fabF*
146 mutation in both suppressor strain backgrounds could suggest that few FabF point
147 modifications would allow both FASII activity and Δ*plsX* complementation.

148 We attempted to prove that the *fabF* mutation was directly responsible for the Δ*plsX*
149 suppressor phenotype by PCR-amplifying the WT *fabF* and mutant *fabF1* alleles, cloning on a
150 medium copy-number vector and constitutive promoter, and establishing plasmids in the
151 Δ*plsX* and/or *fabF1*Δ*plsX* strains, with the goal of reversing the suppressor phenotype. A
152 clone expressing *fabF1*, but not WT *fabF* could be established in the WT RN-R strain by direct
153 transformation.; this is consistent with the putative reduced activity of this allele. We further
154 failed to establish the *fabF1* clone in the Δ*plsX* background, even in FA-supplemented
155 medium. This suggested that *fabF* overexpression was toxic in *S. aureus*, as reported in
156 *Escherichia coli* [17], and that our strategy was not feasible.

157 As an alternate approach, we used a FabF inhibitor, platensimycin, to determine
158 whether disabling FabF was responsible for Δ*plsX* suppression. This antibiotic binds to the
159 acyl-ACP-FabF intermediate, and competes with malonyl-ACP entry, thus preventing FA
160 elongation [18]. However, it also leads to increased levels of FabF and other FASII enzymes
161 in *Bacillus subtilis* [19]. We tested platensimysin, like the FabF mutant, would overcome the
162 Δ*plsX* growth defect, presumably by slowing FabF activity. RN-R Δ*plsX* cultures were plated
163 on BHI solid medium, and platensimycin (1.5 µg) was deposited on plates, which were then

164 incubated 96 h at 37°C (**Fig. 2A**, right plate). In addition to the emergence of Δ*plsX*
165 suppressors, a distinct homogeneous growth ring appeared around the platensimycin spots.
166 Similar experiments were performed in liquid medium using 2-fold dilutions of platensimycin
167 concentrations ranging from 1 ng to 500 ng/ml (**Supplementary Fig. S3**). Compared to BHI
168 medium, growth between 7 and 12 h was significantly stimulated by the presence of 125
169 ng/ml platensimycin (P=≤0.05). However, experiments in liquid medium are potentially
170 flawed as mutant emergence and platensimycin stimulation cannot be distinguished. Ring
171 formation on solid medium appears to be a more accurate means of assessing growth
172 stimulation. Since the *fabF* mutants and a FabF inhibitor both restore Δ*plsX* growth, we
173 consider it likely that the FabF mutation is directly responsible for Δ*plsX* suppression.
174 Reducing *fabF* efficacy by mutation or subinhibitory platensimycin treatments could
175 destabilize the FabF-acyl-ACP intermediate, to liberate free FAs and complement the Δ*plsX*
176 growth defect (**Fig. 2B**).
177
178 **FA auxotrophy of *S. aureus* Δ*plsX* mutants is suppressed by mutations in *fadM* that map to**
179 **the acyl-CoA binding cavity.** We searched for mutations that conferred Δ*plsX* growth on BHI
180 among the 17 remaining suppressors carrying a wild type *fabF* sequence. Genomic DNA
181 sequencing was performed on three such isolates (one derived from RN-R Δ*plsX* and two
182 from JE2 Δ*plsX* backgrounds). A single common gene target, SAOUHSC_01348 in RN-R or
183 SAUSA300_1247 in JE2, was mutated (**Table S1**, **Table S2**). While annotated as a 1,4-
184 dihydroxy-2-naphthoyl-coenzyme A (DHNA-CoA) thioesterase implicated in menaquinone
185 synthesis, the enzyme was shown to have acyl-CoA thioesterase activity [20]. Moreover, the
186 155-amino-acid ORF shares ~40% similarity and a conserved serine, histidine and aspartic
187 acid catalytic triad with FadM, an *E. coli* acyl-CoA thioesterase and ACP binding protein (PBD
188 database protein 1NJK), [20-24]. The *S. aureus* gene, referred to as *fadM*, was PCR-amplified
189 and sequenced in the 17 other suppressors lacking mutations in *fabF*. All carried mutations
190 in *fadM*. A single variant (FadM^{Y90F}, [encoded by *fadM2*]) was identified in the four isolates
191 selected from RN-R Δ*plsX*; three distinct FadM variants were identified among the JE2 Δ*plsX*
192 suppressors (FadM^{I38T} [*fadM1*], FadM^{Y90F} [*fadM2*], and FadM^{Y133F} [*fadM3*]) (**Table S1**, **Table**
193 **S2**). These results point to FabF and FadM as the main suppressors rescuing Δ*plsX* growth.
194 The *S. aureus* FadM crystal structure (PDB: 6FDG) and Alphafold predictions
195 (https://alphafold.ebi.ac.uk/entry/A0A0H2XFE3) provide detailed information for mapping
196 the identified FadM variants conferring Δ*plsX* suppression. The variants coincided with or

197 mapped adjacent to amino acids reportedly involved in forming an FA binding cavity that
198 favors long FA substrates [20] (**Fig. 3A**). The grouped location of these variants leads us to
199 speculate that acyl-CoA thioesterase activity may be defective in the *fadM* suppressors.
200 If FadM acyl-CoA thioesterase activity were needed for Δ*plsX* suppression, then its
201 substrate, acyl-CoA, would need to be produced. In *S. aureus*, acyl-CoA is synthesized by acyl-
202 CoA synthetase (encoded by *fadE*), which is part of the recently elucidated FA degradation
203 (*fad*) system (**Fig. 1**; [25, 26]). The *fad* genes are subject to CcpA-mediated glucose repression
204 [25-27]. However, glucose did not affect the *fadM* mutant Δ*plsX* suppressor phenotypes
205 (**Supplementary Fig. S4**). Based on above results, we consider it reasonable to rule out a role
206 for FadM acyl-CoA thioesterase activity in Δ*plsX* growth rescue.
207
208 **A *fadM* null mutant does not confer Δ*plsX* growth.** Suppression by *fadM* point mutants could
209 be due to FadM-mediated ACP binding, or to the loss of all FadM activity. We asked whether
210 inactivation of *fadM*, the downstream gene in a 2-gene operon comprising *acnA* ([27];
211 **Supplementary Fig. S1**), suppresses the Δ*plsX* phenotype. For this, a *fadM* transposon
212 insertion from the Nebraska Transposon Mutant Library library, interrupting FadM at amino
213 acid position 5, was transferred by ϕ80-mediated transduction into the JE2 Δ*plsX fadM2*
214 suppressor (strain 7.1; **Table S2**) [28]. The Δ*plsX fadM::*Tn strain failed to grow on FA-free
215 medium (**Fig. 3B**). Since total loss of FadM does not promote Δ*plsX* suppression, we conclude
216 that some FadM activity is required for *S. aureus* Δ*plsX* suppression. As FadM I38T, Y90F, and
217 Y133F mutations each map to the acyl-CoA thioesterase binding tunnel, we propose that the
218 FadM ACP binding activity is involved in Δ*plsX* suppression (**Fig. 3C**).
219
220 **Impact of Δ*plsX* suppressors on bacterial growth properties.** Growth of Δ*plsX* suppressors
221 was assessed in RN-R and JE2 backgrounds in non-FA-supplemented BHI medium (**Fig. 4A**).
222 The initial Δ*plsX* deletion strains fail to grow unless supplemented with FAs. Both *fabF* and
223 *fadM* suppressor mutants grew similarly, but their growth phenotypes differed according to
224 the parental strains: in the RN-R background, growth of both tested suppressors was
225 intermediate between the WT strain and the Δ*plsX* mutant. In contrast, JE2 derivative
226 suppressors grew like the parental strain. A distinguishing feature between the two *S. aureus*
227 strains is the production of staphyloxanthin pigment by JE2 but not by RN-R (an RN4220
228 derivative), whose hydrophobic long-chain isoprenyl moiety of staphyloxanthin [29] could
229 conceivably stabilize the membrane in suppressor strains. However, reduced pigmentation

230 of Δ*plsX*, and both *fabF* and *fadM* suppressors compared to WT and *fadM::*Tn controls (**Fig.**
231 **4B**), indicate that other factors are involved in improved rescue in the JE2 background.
232
233 **Membrane FAs are shortened in *fabF* and *fadM* suppressors of Δ*plsX*.** We considered that
234 the *fabF1* point mutation in the Δ*plsX fabF1* suppressor strain might alter FabF processivity,
235 suggesting a shift in FASII products. We also asked whether the mutations in *fadM,* encoding
236 a possible FabF partner, might have similar effects. We therefore assessed membrane FA
237 composition of both Δ*plsX* suppressors in RN-R and JE2 backgrounds in medium devoid of
238 FAs (**Fig. 4C**, **Table S3**). The *fabF* suppressors produced membrane FAs of markedly shorter
239 overall length in both strain backgrounds. Notably, straight-chain FAs C18:0 and C20:0,
240 represent 23-29% of total FAs in parental strains but are essentially absent in *fabF*
241 suppressors. This suggests that processivity of $FabF^{A119E}$ expressed from the *fabF1* suppressor
242 allele is reduced compared to WT FabF. In *S. aureus*, branched chain precursors are preferred
243 substrates for FabH (see **Fig. 1**; [30]), which might lead to higher proportions of branched
244 chain FAs (*ai*15 and *ai*17) in *fabF1* suppressors. FA profiles in the *fadM2* suppressor showed
245 a 2-fold decrease in proportions of C18:0 and C20:0 compared to those in the respective
246 parental strains (**Fig. 4C**, **Table S3**). These results confirm that both *fabF* and *fadM* mutant
247 suppressors of Δ*plsX* lead to decreased proportions of long chain saturated FAs in
248 phospholipids.
249
250 **Δ*plsX* suppressors display accrued β-lactam sensitivity.** β-lactam resistance of methicillin
251 resistant *S. aureus* (MRSA) is associated with the presence of penicillin binding protein
252 Pbp2A' (encoded by *mecA*), and is a main cause of treatment failure [31, 32]. Interestingly,
253 disturbance of membrane lipid microdomains affects Pbp2A' oligomerization and
254 compromises resistance [33]. We asked whether the membrane changes induced by Δ*plsX*
255 suppressors, notably their shorter FAs (**Fig. 4C**) might also impact β-lactam antibiotic
256 resistance profiles. For this, amoxicillin minimal inhibitory concentrations (MICs) were
257 measured by Etests. Tests were performed on BHI solid medium without and with 2.5 µM
258 C18:1; the FA addition allowed us to include Δ*plsX* in these comparisons (**Supplementary Fig.**
259 **S5**). Control strains (WT, *fadM::*Tn, and Δ*plsX*) showed comparable resistance to amoxicillin
260 in both media (0.25-0.38 µg/ml by eTest). Remarkably, all Δ*plsX* suppressors, carrying *fabF*
261 or *fadM* mutant alleles, showed accrued sensitivity, with similar antibiotic resistance
262 phenotypes (0.064-0.094 µg/ml).

263
264 **Acyl-ACP species vary in JE2 WT, Δ*plsX*, and Δ*plsX* suppressors.** Since PlsX uses acyl-ACP, the
265 FASII end product, to initiate phospholipid production, its deletion provokes acyl-ACP
266 accumulation (**Fig. 1**; [5, 34]). Exogenous FA addition resolves accumulated acyl-ACP in a
267 Δ*plsX* mutant [12]. We assessed acyl-ACP intermediate accumulation in the JE2 Δ*plsX* mutant
268 and derivative suppressors by non-denaturing polyacrylamide gel electrophoresis, and
269 probing with anti-ACP antibodies [7, 35] (**Fig. 4D**). Unlike the WT strain, the Δ*plsX* mutant was
270 distinguished by the presence of a fast-migrating band corresponding to ACP bound to long-
271 chain FA generated by FASII, likely the dominant FA *ai*15. The Δ*plsX* strain assimilates acyl-
272 ACP to form phosphatidic acid (PA) only if an exogenous FA (e.g. C18:1) is added to complete
273 PA synthesis (**Fig. 1**). The long acyl-ACP species was absent in Δ*plsX fabF1* and Δ*plsX fadM1,*
274 *M2*, or *M3* suppressors. This observation, and good growth of suppressor strains (**Fig. 4A**)
275 indicate that acyl-ACP is processed to initiate phospholipid synthesis and bypass the
276 phospholipid synthesis block in Δ*plsX*.
277
278 **Δ*plsX* suppressors do not compensate reverse PlsX activity, which is required to bypass the**
279 **FASII pathway.** The above results show that *fabF* and/or *fadM* suppressors compensate the
280 absence of PlsX in normal growth conditions, i.e., in converting acyl-ACP into acyl-PO_4. We
281 asked whether *fabF* and/or *fadM* suppressor strains could also complement the reverse PlsX
282 activity, i.e., conversion of acyl-PO_4 to acyl-ACP (**Fig. 1, Fig. 5A**). If this were the case, FASII
283 inhibition in Δ*plsX* suppressors would be bypassed by FA supplementation to growth
284 medium. To test this, WT strain JE2, and isogenic Δ*plsX*, Δ*plsX fabF1*, and Δ*plsX fadM2* strains
285 were grown in FA-supplemented medium (SerFA, containing 250µM of an FA mixture and
286 10% fetal calf serum; see Materials and Methods), without and with the FASII inhibitor AFN-
287 1252 [36] (**Fig. 5B**). All strains grew to equivalent densities in the absence of inhibitor. The
288 JE2 WT strain overcame the presence of AFN-1252 in SerFA [6, 8]. In contrast, neither the
289 Δ*plsX* mutant nor the Δ*plsX* suppressors could bypass the FASII inhibitor. These findings show
290 that *fabF* or *fadM* suppressor mutations do not compensate the PlsX reverse reaction, and
291 that FASII must be active for Δ*plsX* suppressor growth.
292 As the Δ*plsX fabF* and *fadM* suppressors behaved similarly in all the above phenotypic tests
293 (Figs. 4,5, S4, and S5), we considered that these alleles might cooperate in a single pathway.
294
295 **FadM is required for emergence of Δ*plsX* suppressors mapping to FabF.** As *fadM*
296 interruption abolished Δ*plsX* suppression (**Fig. 3**), we reasoned that suppressors arising in the

297 Δ*plsX fadM::*Tn mutant would map to *fabF*. This hypothesis was tested by comparing
298 suppressor emergence in JE2 Δ*plsX* and Δ*plsX fadM::*Tn backgrounds on solid medium
299 without FA supplementation. We also tested for a stimulatory effect of the FabF inhibitor
300 platensimycin as seen for the Δ*plsX* mutant (**Fig. 2**). Unexpectedly, no suppressors arose after
301 extended (> 1 week) plate incubation at 37°C, compared to frequent mutant emergence in
302 the Δ*plsX* background after 1-2 days (**Fig. 6A, upper**). Moreover, no stimulatory growth ring
303 was detected surrounding the platensimycin spot (**Fig. 6A, lower**). These results affirm that
304 FadM is needed to obtain FabF suppressors of Δ*plsX*. Finally, we introduced the *fadM::*Tn
305 allele into the Δ*plsX fabF1* suppressor mutant. Compared to good growth of Δ*plsX fabF1*,
306 introduction of the *fadM::*Tn allele arrested grow in the absence of exogenous FA, proving
307 that *fadM* is required for *fabF1* rescue (**Fig. 6B**).
308 The potential relevance of FabF-FadM cooperation was examined in a WT background by
309 comparing platensimycin inhibition zones in the WT and *fadM::*Tn derivative on BHI medium
310 (**Supplementary Fig. S6**). While inhibitory zones were equivalent, the WT strain displayed a
311 distinct growth ring (24 h incubation) that is not formed in the *fadM::*Tn mutant. Growth ring
312 rescue from the anti-FabF platensimycin inhibitor also requires FadM in the WT background.
313 Based on all the above findings, we conclude that FadM and FabF have cooperative roles.
314
315
316
317 **Discussion**
318
319 *S. aureus* requires the phospholipid synthesis enzyme PlsX for growth when FAs are not
320 available in its environment. Here, we show that mutations affecting either of two proteins,
321 FabF (a FASII core enzyme), or FadM (a bifunctional protein with acyl-CoA thioesterase and
322 ACP binding activities), allow *S. aureus* to grow even without this essential enzyme [20, 23,
323 27]. To explain growth rescue, we propose that the $FabF^{A119E}$ variant Is responsible for
324 premature release of the FA-ACP intermediate. This explanation is consistent with the
325 shortened FAs in membrane phospholipids and with Δ*plsX* growth stimulation by low anti-
326 FabF concentrations. The FadM I38T, Y90F, Y133F variants all map to the acyl binding tunnel
327 as based on crystallographic and biochemical evidence, and likely impair acyl-CoA
328 thioesterase activity [20, 37]. A functional connection is established between FabF and FadM,
329 as both alleles must be present in order to obtain Δ*plsX* suppressors. Interestingly, all tested

330 phenotypes of the *fabF* and *fadM* suppressors, e.g., growth kinetics, membrane FA
331 shortening, and antibiotic sensitivities, were similar. While the nature of FabF-FadM
332 cooperation, whether direct or indirect, remains to be elucidated, these results identify FadM
333 as a key modulator linking FASII and phospholipid homeostasis in *S. aureus*.

334 We propose a working model to explain Δ*plsX* growth rescue by FabF and FadM variants
335 [38] (**Fig. 7**). In this model, the $FabF^{A119E}$ variant (or FabF in the presence of subinhibitory
336 amounts of platensimycin) may stall and release its FA-ACP cargo before malonyl-ACP entry,
337 which is needed for FA elongation. ACP binding by FadM would facilitate ACP removal from
338 the FabF cavity, thus favoring FA release. The FA made available would then be
339 phosphorylated by Fak for entry into the phospholipid synthesis pathway.
340 FadM suppressor variants with modifications in their FA-binding cavity are predicted to
341 exhibit reduced acyl-CoA thioesterase activity, as previously observed [20] and proposed
342 here. This would increase the availability of FadM to facilitate ACP removal and FA release
343 from the FabF intermediate. In contrast, a FadM null mutation would exclude this process,
344 consistent with our findings that *fadM* is required for Δ*plsX* suppression.
345 The newly uncovered contribution of FadM to FabF activity may have relevance to WT *S.*
346 *aureus* FASII-phospholipid homeostasis by acting as an FA release valve that decreases FabF
347 processivity, leading to shortened phospholipid FAs, e.g., under stress conditions. This
348 hypothesis is currently being investigated.
349 Remarkably, the Δ*plsX* suppressor strains are β-lactam-sensitive as compared to the MRSA
350 JE2 parent or its Δ*plsX*, and *fadM::*Tn derivatives (**Supplementary Fig. S5**). Both *fabF* and
351 *fadM* suppressors display similar greater amoxicillin sensitivity, as expected if FabF and FadM
352 act on the same pathway. The mechanisms underlying β-lactam-sensitivity and the potential
353 role of membrane synthesis or composition remain unclear, but may involve destabilization
354 of PBP2', as reported [33]. Thus, rerouting phospholipid synthesis rescues *S. aureus* Δ*plsX*
355 growth but reduces the bacterial response to β-lactam antibiotics. These observations open
356 perspectives for understanding how membrane perturbations, as occur in Δ*plsX* suppressor
357 strains, might resensitize bacteria to this important class of antibiotics.
358
359

360 **Materials and methods**

361

362 **Strains, growth conditions, and plasmids.** Strains and plasmids are listed in **Table S4**. *S.*
363 *aureus* strains are derived from USA300_FPR3757 strain JE2 [28] and RN4220-R (called here
364 RN-R; [15]). RN-R is a readily transformable strain derived from RN4220, of the NCTC 8325
365 lineage [39]. It was repaired to restore a functional *fakB1* gene, which is defective in the
366 entire NCTC 8325 lineage [15]). *S. aureus* parental strains and Δ*plsX*-suppressor mutants were
367 grown in BHI medium (Brain Heart Infusion; Gibco, France) or in LB (Lysogeny broth; [40]) as
368 specified, at 37°C with shaking. Medium was supplemented with C18:1 (oleic acid) at a
369 concentration of 250 µM (Larodan, Sweden) when indicated. The FabI inhibitor AFN-1252
370 (Med ChemExpress, France) and FabF inhibitor platensimycin (Bioaustralis-Tebubio France)
371 were used as specified [18, 41].

372 **Δ*plsX* mutant construction.** The Δ*plsX* mutants were constructed in RN-R (RN4220 repaired
373 for a defective *fakB1* gene in the NCTC8325 lineage; [15]) and JE2 backgrounds. The
374 preparatory plasmid for *plsX* deletion was constructed using the Gibson assembly method to
375 insert DNA segments flanking the *plsX orf* into Sma1-linearized pMAD, a thermosensitive
376 plasmid expressing erythromycin resistance [42, 43]. Oligonucleotides for Δ*plsX* construction
377 are in **Table S5**. Constructions were verified by DNA sequencing of PCR-amplified fragments.
378 The double cross-over gene replacements were obtained as described [15, 43] in RN-R and
379 JE2 strains. Deletions removed nucleotides 1,228,616-1,229,594 in JE2, and 1,148,670-
380 1,149,648 in RN-R, as per respective annotated genomes. The resultant strain genotypes
381 were confirmed by whole genome sequencing (Eurofins, Germany).

382 ***plsX* cloning and complementation of the Δ*plsX* mutant in RN-R and JE2 strains.** To confirm
383 that strain characteristics were due to the *plsX* deletion, the intact *plsX* gene was cloned with
384 its natural promoter (upstream of *fapR*) on multicopy plasmid pIM-locus1 (a pIMAY
385 derivative [44, 45]). Cloning was performed by Gibson assembly with oligonucleotide primers
386 (**Table S5**).

387 **Isolation of suppressor mutants.** RN-R Δ*plsX* and JE2 Δ*plsX* strains were first streaked on solid
388 BHI medium containing 250 µM C18:1, an FA that promotes growth. For each strain, a single
389 colony was used to inoculate a liquid culture (in BHI+C18:1). When the culture reached
390 exponential phase, bacteria were centrifuged, resuspended in BHI, and adjusted to OD_{600} =
391 0.1. Dilutions were plated on solid medium to obtain ~10^5 to ~10^7 colony forming units per
392 plate on solid BHI medium without FAs. Colonies were scored after two or more days of

393 incubation at 37°C, and selected at random for restreaking on solid BHI medium. Liquid
394 cultures were prepared in BHI, and stocked in 20% glycerol for storage at -70°C. Selected
395 mutant genotypes were confirmed by whole genome sequencing or by PCR fragment
396 sequencing (Eurofins, Germany) to identify mutated loci.
397 **Genomic DNA preparation for whole genome sequencing.** Bacterial cell pellets, prepared
398 from 3 mL liquid exponential phase cultures, were centrifuged at 8,000 rpm for 5 min. Pellets
399 were re-suspended in 800 µL Tris-EDTA buffer (10 mM Tris- HC1, pH 8.0/1 mM EDTA) plus 20
400 µL lysostaphin 5 mg/mL, and incubated for 45 min at 37°C. DNA was prepared by DNeasy
401 Blood & Tissue Kit (Qiagen, France) and samples were outsourced for whole genome DNA
402 sequencing using 2x150 bp paired end chemistry and bioinformatics analyses (Eurofins
403 Genomics, France) [6]. SNPs that differed in non-antibiotic-treated JE2 and RN-R strains from
404 those in the reference sequence (GenBank Nucleotide accession codes NC_007793.1 and
405 NC_007795.1 respectively) were subtracted prior to variant identification. Variants were
406 identified as representing ≥80% of reads in sequences for which there were at least 100
407 reads.
408 **PCR amplification and confirmation by DNA sequencing.** Selected candidate colonies were
409 suspended in 100 µL of 0.9% NaCl with 1 µL of lysostaphin from a 5 mg/mL stock. Tubes
410 containing suspensions were shaken for 45 min at 37°C. Contents were then transferred to
411 tubes containing glass beads and samples were vortexed for 1 min. After a 30 second
412 centrifugation at 8000 rpm, PCR amplification was performed on 1 µl of supernatant, using
413 primers (**Table S5**) and Phusion DNA polymerase (ThermoFisher Scientific, France) according
414 to manufacturer protocol, using a SimpliAmp Thermal Cycler (ThermoFisher Scientific,
415 France). PCR products were analyzed on a 0.8% agarose gel prepared in 40 mM Tris acetate
416 1 mM EDTA buffer containing 0.5 µg/mL ethidium bromide. Gels were run at 100 V for 30
417 min in an electrophoresis chamber (Mupid ONE; Dutscher, France), and photographed under
418 UV light using the EBOX VX5 imaging system (Vilber Lourmat, France). PCR samples were
419 purified using the NucleoSpin® Gel and PCR Clean-up kit (Macherey-Nagel, France), and sent
420 for DNA sequencing (Eurofins, France).
421 **Effects of the FabF inhibitor platensimycin on Δ*plsX* and Δ*plsX fadM::*Tn strains.** Strains
422 were grown in BHI containing C18:1 (250 µM) overnight, washed once in BHI medium, and
423 resuspended in BHI to a final density of OD_{600} = 0.1. From this, 100 µl of the bacterial
424 suspension was plated on solid BHI medium. Platensimycin (1.5 µg in 3 µl) was spotted in the
425 center of plates, which were then incubated at 37°C for 4-7 days and photographed.

426 **Effect of glucose on growth of Δ*plsX* suppressors.** Strains were precultured in liquid LB (n.b.,
427 LB lacks glucose) or LB with C18:1 for Δ*plsX* at 37°C. After overnight growth, cultures were
428 diluted to OD_{600} = 0.05 and grown for 3-4 hours. Δ*plsX* cultures were first centrifuged and
429 resuspended in fresh LB medium to remove free FAs prior to regrowth. Bacterial densities
430 were then adjusted to OD_{600} = 1. Cultures were streaked on solid medium, corresponding to
431 LB or LB containing 0.5% glucose, which represses *fad* operon expression [25, 27]. Plates were
432 incubated at 37°C for 24 hours and photographed.
433 **Growth kinetics.** Three mL precultures were prepared in BHI for parental and Δ*plsX*
434 suppressor strains, or in BHI containing 250 µM C18:1 for Δ*plsX* mutants. After overnight
435 growth, culture OD_{600} were adjusted to OD_{600} = 0.05 in 200 µL BHI medium without or with
436 C18:1 (250 µM), in 96-well microtiter plates. Growth was followed on a Spark M10 plate
437 reader (Tecan, France). For experiments in which samples were taken for FA determinations
438 or for Western blot experiments, cultures were prepared in 3 to 10 ml liquid cultures, and
439 were monitored manually by OD_{600} measurements every two hours. Amoxicillin sensitivity
440 was determined using AMOXICILLIN AC 256 eTests (BioMérieux, France).
441 **Determination of membrane FA profiles.** Bacterial cultures (equivalent of OD_{600} = 2) were
442 centrifuged, and pellets were washed once in 1 ml of 0.02% Triton in 0.9% NaCl, then twice
443 with 1 ml of 0.9% NaCl. FA extractions were performed as described [46] [6]. Briefly, 0.5 mL
444 of 1N sodium methoxide in methanol was added to bacterial pellets in 2 ml microfuge tubes,
445 and then subjected to a 5 min ultrasound bath. Then 0.2 mL heptane spiked with methyl-10-
446 undecenoate (Sigma-Aldrich) as internal standard was added, followed by 1 min vortexing,
447 and short centrifugation for phase separation. FA methyl esters were recovered in the
448 heptane phase. Analyses were performed in a split-splitless injection mode on an
449 AutoSystem XL Gas Chromatograph (Perkin-Elmer) equipped with a ZB-Wax capillary column
450 (30 m x 0.25 mm x 0.25 µm; Phenomenex, France). Data were recorded and analyzed by
451 TotalChrom Workstation (Perkin-Elmer). *S. aureus* FA peaks were detected between 12 and
452 32 min of elution, and identified with retention times of purified esterified FA standards.
453 **Detection of ACP products.** Pellets from OD_{600}=10 equivalent of exponential phase cultures
454 were collected by centrifugation (8000 rpm for 5 min), and then washed twice with PBS
455 (Phosphate Buffer Saline)-Triton X100 0.1%, and once with PBS. Pellets were re-suspended
456 in 600 µL PBS supplemented with 6 µL antiprotease (100X), 50 µg/mL lysostaphin and 50
457 µg/mL DNAse and incubated with shaking for 25 min at 37°C. Protein concentrations were
458 determined [47], and extracts (10 µg) were loaded onto non-denaturing gels containing 1M
459 urea and 14% acrylamide gel as described [5, 7]. After electrophoresis, gels were subject to

460 electroblotting for transfer to a PVDF membrane (Biorad, France) using a current of 25 V and
461 1.3 A on a power blotter semi-dry transfer system (Invitrogen, France) for 7 min. Primary
462 anti-ACP antibody (Covalabs, France; [7]) was used at 1:500 dilution and secondary anti-
463 rabbit IgG conjugated with peroxidase (Invitrogen, France) at a 1:5000 dilution. ACP-reactive
464 bands were identified using the ECL kit (Perkin Elmer, France) and the fluorescent signal was
465 recorded using ChemiDoc (BioRad, France).
466 **Phage transductions.** Transductions of *fadM::*Tn transposon insertion from JE2 into Δ*plsX*
467 suppressors *fadM2* and *fabF1* were performed as described using ϕ80 phage stock [48] [49].
468 The *fadM* transposon insertion [28] was transduced into JE2 Δ*plsX fadM2* suppressor strain
469 7.1 and into JE2 Δ*plsX fabF1* suppressor strain 7.8, giving rise respectively to Δ*plsX fadM::*Tn
470 and Δ*plsX fabF1 fadM::*Tn, using erythromycin (5 µg/ml) as selection (**Table S4**). Insertions
471 were confirmed by PCR.
472 **FASII bypass of WT and Δ*plsX* derivative strains.** Anti-FASII bypass was evaluated as
473 described [6]. Strains were grown overnight in liquid SerFA medium (SerFA, BHI containing
474 10 % newborn calf serum and an equimolar mixture of 83 µM each C14:0, C16:0, and C18:1
475 [Larodan, Sweden]). Cultures were then diluted to OD_{600}=0.05 in SerFA containing or not 0.5
476 µg/ml of the anti-FASII AFN-1252 (here called AFN; [36]; MedChemExpress, France). Growth
477 was monitored using the Spark plate reader (Tecan, France).
478 **Whole-genome sequencing data of S. aureus Δ*plsX* mutants and suppressors.** Data is
479 available in the Mendeley database: DOI: 10.17632/mzw2429w3m.1 .
480

481 **Acknowledgements and funding**

482 We are grateful to Kam Pou Han and Philippe Bouloc (Bouloc lab, I2BC, Orsay, France) for
483 providing transducing phage and plasmid; Florence Dubois-Brissonet and Katia de Oliveira
484 (Micalis, INRAE) for expert help and advice with CpG analyses; Candice Rigoulay for a
485 simplified phage transduction protocol. We thank Micalis Institute colleagues Vincent Juillard
486 for discussion of PlsX functions, and Philippe Gaudu, Jasmina Vidic, and team members for
487 stimulating discussion and pertinent comments. We thank the PAPPSO proteomics facility
488 (https://doi.org/10.15454/1.5572393176364355E12 ; supported by Paris-Saclay University,
489 INRAE, AgroParisTech, the Ile-de-France Regional Council, and the IBiSA network) for an
490 exploratory study that inspired β-lactam sensitivity testing.
491 This work was supported by the French Agence Nationale de la Recherche ANR (ANR-16-
492 CE15-0013; AG), the Joint Programming Initiative on Antimicrobial Resistance (JPIAMR)

under the umbrella of the ANR (ANR-22-AAMR-0007; AG), and the Fondation pour la Recherche Medicale (DBF20161136769; AG). PW was recipient of a Franco-Thai scholarship from Campus France and Khon Kaen University.

Data availability

All relevant data are within the manuscript, supporting information files, and repositories. Any biological materials are available upon request.

Author Contributions

All authors performed, analyzed, and interpreted experiments, and approved the manuscript. PW, JAM, and AG conceived the project, designed research, and wrote the paper.

Competing interests

The authors declare no competing interests.

513 **References**
514
515 1. Zhang YM, Rock CO. Membrane lipid homeostasis in bacteria. Nat Rev Microbiol.
516 2008;6(3):222-33. Epub 2008/02/12. doi: 10.1038/nrmicro1839. PubMed PMID: 18264115.
517 2. Silbert DF, Ruch F, Vagelos PR. Fatty acid replacements in a fatty acid auxotroph of
518 *Escherichia coli*. J Bacteriol. 1968;95(5):1658-65. Epub 1968/05/01. doi: 10.1128/jb.95.5.1658-
519 1665.1968. PubMed PMID: 4870280; PubMed Central PMCID: PMCPMC252192.
520 3. Lu YJ, Zhang YM, Grimes KD, Qi J, Lee RE, Rock CO. Acyl-phosphates initiate membrane
521 phospholipid synthesis in Gram-positive pathogens. Mol Cell. 2006;23(5):765-72. Epub 2006/09/05.
522 doi: 10.1016/j.molcel.2006.06.030. PubMed PMID: 16949372.
523 4. Parsons JB, Broussard TC, Bose JL, Rosch JW, Jackson P, Subramanian C, et al. Identification
524 of a two-component fatty acid kinase responsible for host fatty acid incorporation by
525 *Staphylococcus aureus*. Proc Natl Acad Sci U S A. 2014;111(29):10532-7. Epub 2014/07/09. doi:
526 10.1073/pnas.1408797111. PubMed PMID: 25002480; PubMed Central PMCID: PMCPMC4115530.
527 5. Parsons JB, Frank MW, Jackson P, Subramanian C, Rock CO. Incorporation of extracellular
528 fatty acids by a fatty acid kinase-dependent pathway in *Staphylococcus aureus*. Mol Microbiol.
529 2014;92(2):234-45. doi: 10.1111/mmi.12556. PubMed PMID: 24673884; PubMed Central PMCID:
530 PMC4007170.
531 6. Kenanian G, Morvan C, Weckel A, Pathania A, Anba-Mondoloni J, Halpern D, et al.
532 Permissive Fatty Acid Incorporation Promotes Staphylococcal Adaptation to FASII Antibiotics in
533 Host Environments. Cell Rep. 2019;29(12):3974-82 e4. Epub 2019/12/19. doi:
534 10.1016/j.celrep.2019.11.071. PubMed PMID: 31851927.
535 7. Morvan C, Halpern D, Kenanian G, Hays C, Anba-Mondoloni J, Brinster S, et al.
536 Environmental fatty acids enable emergence of infectious *Staphylococcus aureus* resistant to FASII-
537 targeted antimicrobials. Nat Commun. 2016;7:12944. doi: 10.1038/ncomms12944. PubMed PMID:
538 27703138; PubMed Central PMCID: PMC5059476.
539 8. Wongdontree P, Millan-Oropeza A, Upfold J, Lavergne JP, Halpern D, Lambert C, et al.
540 Oxidative stress is intrinsic to staphylococcal adaptation to fatty acid synthesis antibiotics. iScience.
541 2024;27(4):109505. Epub 2024/04/05. doi: 10.1016/j.isci.2024.109505. PubMed PMID: 38577105;
542 PubMed Central PMCID: PMCPMC10993138.
543 9. Sastre DE, Pulschen AA, Basso LGM, Benites Pariente JS, Marques Netto CGC,
544 Machinandiarena F, et al. The phosphatidic acid pathway enzyme PlsX plays both catalytic and
545 channeling roles in bacterial phospholipid synthesis. J Biol Chem. 2020;295(7):2148-59. Epub
546 2020/01/11. doi: 10.1074/jbc.RA119.011147. PubMed PMID: 31919098; PubMed Central PMCID:
547 PMCPMC7029103.
548 10. Rex AN, Simpson BW, Bokinsky G, Trent MS. PlsX and PlsY: Additional roles beyond
549 glycerophospholipid synthesis in Gram-negative bacteria. mBio. 2024:e0296924. Epub 2024/10/30.
550 doi: 10.1128/mbio.02969-24. PubMed PMID: 39475235.
551 11. Jing F, Cantu DC, Tvaruzkova J, Chipman JP, Nikolau BJ, Yandeau-Nelson MD, et al.
552 Phylogenetic and experimental characterization of an acyl-ACP thioesterase family reveals
553 significant diversity in enzymatic specificity and activity. BMC Biochem. 2011;12:44. Epub
554 2011/08/13. doi: 10.1186/1471-2091-12-44. PubMed PMID: 21831316; PubMed Central PMCID:
555 PMCPMC3176148.
556 12. Parsons JB, Frank MW, Eleveld MJ, Schalkwijk J, Broussard TC, de Jonge MI, et al. A
557 thioesterase bypasses the requirement for exogenous fatty acids in the *plsX* deletion of

558 *Streptococcus pneumoniae*. Mol Microbiol. 2015;96(1):28-41. Epub 2014/12/24. doi:
559 10.1111/mmi.12916. PubMed PMID: 25534847; PubMed Central PMCID: PMCPMC4415690.
560 13. Zou Q, Dong H, Cronan JE. Growth of *Enterococcus faecalis* Δ*plsX* strains is restored by
561 increased saturated fatty acid synthesis. mSphere. 2023;8(4):e0012023. Epub 2023/06/08. doi:
562 10.1128/msphere.00120-23. PubMed PMID: 37289195; PubMed Central PMCID:
563 PMCPMC10449490.
564 14. Cross B, Garcia A, Faustoferri R, Quivey RG. PlsX deletion impacts fatty acid synthesis and
565 acid adaptation in *Streptococcus mutans*. Microbiology (Reading). 2016;162(4):662-71. Epub
566 2016/02/07. doi: 10.1099/mic.0.000252. PubMed PMID: 26850107; PubMed Central PMCID:
567 PMCPMC4892098.
568 15. Pathania A, Anba-Mondoloni J, Gominet M, Halpern D, Dairou J, Dupont L, et al.
569 (p)ppGpp/GTP and Malonyl-CoA Modulate *Staphylococcus aureus* Adaptation to FASII Antibiotics
570 and Provide a Basis for Synergistic Bi-Therapy. mBio. 2021;12(1). Epub 2021/02/04. doi:
571 10.1128/mBio.03193-20. PubMed PMID: 33531402; PubMed Central PMCID: PMCPMC7858065.
572 16. Rashid R, Nair ZJ, Chia DMH, Chong KKL, Cazenave Gassiot A, Morley SA, et al. Depleting
573 Cationic Lipids Involved in Antimicrobial Resistance Drives Adaptive Lipid Remodeling in
574 *Enterococcus faecalis*. mBio. 2023;14(1):e0307322. Epub 2023/01/12. doi: 10.1128/mbio.03073-
575 22. PubMed PMID: 36629455; PubMed Central PMCID: PMCPMC9973042.
576 17. Subrahmanyam S, Cronan JE, Jr. Overproduction of a functional fatty acid biosynthetic
577 enzyme blocks fatty acid synthesis in *Escherichia coli*. J Bacteriol. 1998;180(17):4596-602. Epub
578 1998/08/29. doi: 10.1128/JB.180.17.4596-4602.1998. PubMed PMID: 9721301; PubMed Central
579 PMCID: PMCPMC107473.
580 18. Wang J, Soisson SM, Young K, Shoop W, Kodali S, Galgoci A, et al. Platensimycin is a selective
581 FabF inhibitor with potent antibiotic properties. Nature. 2006;441(7091):358-61. doi:
582 10.1038/nature04784. PubMed PMID: 16710421.
583 19. Wenzel M, Patra M, Albrecht D, Chen DY, Nicolaou KC, Metzler-Nolte N, et al. Proteomic
584 signature of fatty acid biosynthesis inhibition available for in vivo mechanism-of-action studies.
585 Antimicrob Agents Chemother. 2011;55(6):2590-6. Epub 2011/03/09. doi: 10.1128/AAC.00078-11.
586 PubMed PMID: 21383089; PubMed Central PMCID: PMCPMC3101464.
587 20. Murad AM, Brognaro H, Falke S, Lindner J, Perbandt M, Mudogo C, et al. Structure and
588 activity of the DHNA Coenzyme-A Thioesterase from *Staphylococcus aureus* providing insights for
589 innovative drug development. Sci Rep. 2022;12(1):4313. Epub 2022/03/14. doi: 10.1038/s41598-
590 022-08281-2. PubMed PMID: 35279696; PubMed Central PMCID: PMCPMC8918352.
591 21. Swarbrick CMD, Nanson JD, Patterson EI, Forwood JK. Structure, function, and regulation
592 of thioesterases. Prog Lipid Res. 2020;79:101036. Epub 2020/05/18. doi:
593 10.1016/j.plipres.2020.101036. PubMed PMID: 32416211.
594 22. Butland G, Peregrin-Alvarez JM, Li J, Yang W, Yang X, Canadien V, et al. Interaction network
595 containing conserved and essential protein complexes in *Escherichia coli*. Nature.
596 2005;433(7025):531-7. Epub 2005/02/04. doi: 10.1038/nature03239. PubMed PMID: 15690043.
597 23. Cherkasov A, Hsing M, Zoraghi R, Foster LJ, See RH, Stoynov N, et al. Mapping the protein
598 interaction network in methicillin-resistant *Staphylococcus aureus*. J Proteome Res.
599 2011;10(3):1139-50. Epub 2010/12/21. doi: 10.1021/pr100918u. PubMed PMID: 21166474.
600 24. Gully D, Bouveret E. A protein network for phospholipid synthesis uncovered by a variant
601 of the tandem affinity purification method in *Escherichia coli*. Proteomics. 2006;6(1):282-93. Epub
602 2005/11/19. doi: 10.1002/pmic.200500115. PubMed PMID: 16294310.

603 25. Kuiack RC, Tuffs SW, Dufresne K, Flick R, McCormick JK, McGavin MJ. The *fadXDEBA* locus
604 of *Staphylococcus aureus* is required for metabolism of exogenous palmitic acid and in vivo growth.
605 Mol Microbiol. 2023;120(3):425-38. Epub 2023/07/28. doi: 10.1111/mmi.15131. PubMed PMID:
606 37501506.
607 26. Menjivar C, DeMars ZR, Wiemels RE, Carroll RK, Bose JL. Characterizing the *Staphylococcus*
608 *aureus* fatty acid degradation operon. J Bacteriol. 2025;207(8):e0008925. Epub 2025/07/17. doi:
609 10.1128/jb.00089-25. PubMed PMID: 40673679; PubMed Central PMCID: PMCPMC12369327.
610 27. Mader U, Nicolas P, Depke M, Pane-Farre J, Debarbouille M, van der Kooi-Pol MM, et al.
611 *Staphylococcus aureus* Transcriptome Architecture: From Laboratory to Infection-Mimicking
612 Conditions. PLoS Genet. 2016;12(4):e1005962. doi: 10.1371/journal.pgen.1005962. PubMed PMID:
613 27035918; PubMed Central PMCID: PMC4818034.
614 28. Fey PD, Endres JL, Yajjala VK, Widhelm TJ, Boissy RJ, Bose JL, et al. A genetic resource for
615 rapid and comprehensive phenotype screening of nonessential *Staphylococcus aureus* genes. MBio.
616 2013;4(1):e00537-12. doi: 10.1128/mBio.00537-12. PubMed PMID: 23404398; PubMed Central
617 PMCID: PMC3573662.
618 29. Pelz A, Wieland KP, Putzbach K, Hentschel P, Albert K, Gotz F. Structure and biosynthesis of
619 staphyloxanthin from *Staphylococcus aureus*. J Biol Chem. 2005;280(37):32493-8. Epub
620 2005/07/16. doi: 10.1074/jbc.M505070200. PubMed PMID: 16020541.
621 30. Qiu X, Choudhry AE, Janson CA, Grooms M, Daines RA, Lonsdale JT, et al. Crystal structure
622 and substrate specificity of the beta-ketoacyl-acyl carrier protein synthase III (FabH) from
623 *Staphylococcus aureus*. Protein Sci. 2005;14(8):2087-94. Epub 2005/07/01. doi:
624 10.1110/ps.051501605. PubMed PMID: 15987898; PubMed Central PMCID: PMCPMC2279320.
625 31. Song MD, Wachi M, Doi M, Ishino F, Matsuhashi M. Evolution of an inducible penicillin-
626 target protein in methicillin-resistant *Staphylococcus aureus* by gene fusion. FEBS Lett.
627 1987;221(1):167-71. Epub 1987/08/31. doi: 10.1016/0014-5793(87)80373-3. PubMed PMID:
628 3305073.
629 32. Antimicrobial Resistance C. Global burden of bacterial antimicrobial resistance in 2019: a
630 systematic analysis. Lancet. 2022;399(10325):629-55. Epub 2022/01/24. doi: 10.1016/S0140-
631 6736(21)02724-0. PubMed PMID: 35065702.
632 33. Garcia-Fernandez E, Koch G, Wagner RM, Fekete A, Stengel ST, Schneider J, et al. Membrane
633 Microdomain Disassembly Inhibits MRSA Antibiotic Resistance. Cell. 2017;171(6):1354-67 e20.
634 Epub 2017/11/07. doi: 10.1016/j.cell.2017.10.012. PubMed PMID: 29103614; PubMed Central
635 PMCID: PMCPMC5720476.
636 34. Machinandiarena F, Nakamatsu L, Schujman GE, de Mendoza D, Albanesi D. Revisiting the
637 coupling of fatty acid to phospholipid synthesis in bacteria with FapR regulation. Mol Microbiol.
638 2020;114(4):653-63. Epub 2020/07/17. doi: 10.1111/mmi.14574. PubMed PMID: 32671874.
639 35. Cronan JE, Thomas J. Bacterial fatty acid synthesis and its relationships with polyketide
640 synthetic pathways. Methods Enzymol. 2009;459:395-433. Epub 2009/04/14. doi: 10.1016/S0076-
641 6879(09)04617-5. PubMed PMID: 19362649; PubMed Central PMCID: PMCPMC4095770.
642 36. Karlowsky JA, Kaplan N, Hafkin B, Hoban DJ, Zhanel GG. AFN-1252, a FabI inhibitor,
643 demonstrates a Staphylococcus-specific spectrum of activity. Antimicrob Agents Chemother.
644 2009;53(8):3544-8. doi: 10.1128/AAC.00400-09. PubMed PMID: 19487444; PubMed Central
645 PMCID: PMC2715641.
646 37. Jumper J, Evans R, Pritzel A, Green T, Figurnov M, Ronneberger O, et al. Highly accurate
647 protein structure prediction with AlphaFold. Nature. 2021;596(7873):583-9. Epub 2021/07/16. doi:
648 10.1038/s41586-021-03819-2. PubMed PMID: 34265844; PubMed Central PMCID:

PMCPMC8371605 have filed non-provisional patent applications 16/701,070 and PCT/EP2020/084238, and provisional patent applications 63/107,362, 63/118,917, 63/118,918, 63/118,921 and 63/118,919, each in the name of DeepMind Technologies Limited, each pending, relating to machine learning for predicting protein structures. The other authors declare no competing interests.

38. Mindrebo JT, Patel A, Kim WE, Davis TD, Chen A, Bartholow TG, et al. Gating mechanism of elongating beta-ketoacyl-ACP synthases. Nat Commun. 2020;11(1):1727. Epub 2020/04/09. doi: 10.1038/s41467-020-15455-x. PubMed PMID: 32265440; PubMed Central PMCID: PMCPMC7138838.

39. Herbert S, Ziebandt AK, Ohlsen K, Schafer T, Hecker M, Albrecht D, et al. Repair of global regulators in *Staphylococcus aureus* 8325 and comparative analysis with other clinical isolates. Infect Immun. 2010;78(6):2877-89. Epub 2010/03/10. doi: 10.1128/IAI.00088-10. PubMed PMID: 20212089; PubMed Central PMCID: PMCPMC2876537.

40. Bertani G. Studies on lysogenesis. I. The mode of phage liberation by lysogenic *Escherichia coli*. J Bacteriol. 1951;62(3):293-300. Epub 1951/09/01. doi: 10.1128/jb.62.3.293-300.1951. PubMed PMID: 14888646; PubMed Central PMCID: PMCPMC386127.

41. Hunt T, Kaplan N, Hafkin B. Safety, tolerability and pharmacokinetics of multiple oral doses of AFN-1252 administered as immediate release (IR) tablets in healthy subjects. Journal of chemotherapy. 2016;28(3):164-71. doi: 10.1179/1973947815Y.0000000075. PubMed PMID: 26431470.

42. Arnaud M, Chastanet A, Debarbouille M. New vector for efficient allelic replacement in naturally nontransformable, low-GC-content, gram-positive bacteria. Appl Environ Microbiol. 2004;70(11):6887-91. Epub 2004/11/06. doi: 10.1128/AEM.70.11.6887-6891.2004. PubMed PMID: 15528558; PubMed Central PMCID: PMCPMC525206.

43. Biswas I, Gruss A, Ehrlich SD, Maguin E. High-efficiency gene inactivation and replacement system for gram-positive bacteria. J Bacteriol. 1993;175(11):3628-35. Epub 1993/06/01. doi: 10.1128/jb.175.11.3628-3635.1993. PubMed PMID: 8501066; PubMed Central PMCID: PMCPMC204764.

44. Coronel-Tellez RH, Pospiech M, Barrault M, Liu W, Bordeau V, Vasnier C, et al. sRNA-controlled iron sparing response in Staphylococci. Nucleic Acids Res. 2022;50(15):8529-46. Epub 2022/07/30. doi: 10.1093/nar/gkac648. PubMed PMID: 35904807; PubMed Central PMCID: PMCPMC9410917.

45. Monk IR, Shah IM, Xu M, Tan MW, Foster TJ. Transforming the untransformable: application of direct transformation to manipulate genetically *Staphylococcus aureus* and *Staphylococcus epidermidis*. mBio. 2012;3(2). Epub 2012/03/22. doi: 10.1128/mBio.00277-11. PubMed PMID: 22434850; PubMed Central PMCID: PMCPMC3312211.

46. Rozes N, Garbay S, Denayrolles M. A rapid method for the determination of bacterial fatty acid composition. Lett Appl Microbiol. 1993;17(3):126-31. doi: https://doi.org/10.1111/j.1472-765X.1993.tb01440.x.

47. Bradford MM. A rapid and sensitive method for the quantitation of microgram quantities of protein utilizing the principle of protein-dye binding. Anal Biochem. 1976;72:248-54. Epub 1976/05/07. doi: 10.1006/abio.1976.9999. PubMed PMID: 942051.

48. Olson ME. Bacteriophage Transduction in *Staphylococcus aureus*. Methods Mol Biol. 2016;1373:69-74. Epub 2015/02/04. doi: 10.1007/7651_2014_186. PubMed PMID: 25646608.

49. Bowring JZ, Su Y, Alsaadi A, Svenningsen SL, Parkhill J, Ingmer H. Screening for Highly Transduced Genes in *Staphylococcus aureus* Revealed Both Lateral and Specialized Transduction.

695 Microbiol Spectr. 2022;10(1):e0242321. Epub 2022/02/10. doi: 10.1128/spectrum.02423-21.
696 PubMed PMID: 35138167; PubMed Central PMCID: PMCPMC8826898.
697 50. Fujita Y, Matsuoka H, Hirooka K. Regulation of fatty acid metabolism in bacteria. Mol
698 Microbiol. 2007;66(4):829-39. Epub 2007/10/09. doi: 10.1111/j.1365-2958.2007.05947.x. PubMed
699 PMID: 17919287.
700 51. Brown ED. Microbiology: antibiotic stops 'ping-pong' match. Nature. 2006;441(7091):293-
701 4. Epub 2006/05/20. doi: 10.1038/441293a. PubMed PMID: 16710404.
702 52. Pettersen EF, Goddard TD, Huang CC, Couch GS, Greenblatt DM, Meng EC, et al. UCSF
703 Chimera--a visualization system for exploratory research and analysis. J Comput Chem.
704 2004;25(13):1605-12. Epub 2004/07/21. doi: 10.1002/jcc.20084. PubMed PMID: 15264254.
705 53. Rock CO, Cronan JE, Jr., Armitage IM. Molecular properties of acyl carrier protein
706 derivatives. J Biol Chem. 1981;256(6):2669-74. Epub 1981/03/25. PubMed PMID: 7009596.
707 54. Cronan JE, Jr. Molecular properties of short chain acyl thioesters of acyl carrier protein. J
708 Biol Chem. 1982;257(9):5013-7. Epub 1982/05/10. PubMed PMID: 7040391.
709 55. Brinster S, Lamberet G, Staels B, Trieu-Cuot P, Gruss A, Poyart C. Type II fatty acid synthesis
710 is not a suitable antibiotic target for Gram-positive pathogens. Nature. 2009;458(7234):83-6. doi:
711 10.1038/nature07772. PubMed PMID: 19262672.
712 56. Kuhn S, Slavetinsky CJ, Peschel A. Synthesis and function of phospholipids in *Staphylococcus*
713 *aureus*. Int J Med Microbiol. 2015;305(2):196-202. Epub 2015/01/18. doi:
714 10.1016/j.ijmm.2014.12.016. PubMed PMID: 25595024.
715 57. Monk IR, Stinear TP. From cloning to mutant in 5 days: rapid allelic exchange in
716 *Staphylococcus aureus*. Access Microbiol. 2021;3(2):000193. Epub 2021/06/22. doi:
717 10.1099/acmi.0.000193. PubMed PMID: 34151146; PubMed Central PMCID: PMCPMC8209637.
718 58. Christie GE, Matthews AM, King DG, Lane KD, Olivarez NP, Tallent SM, et al. The complete
719 genomes of *Staphylococcus aureus* bacteriophages 80 and 80alpha--implications for the specificity
720 of SaPI mobilization. Virology. 2010;407(2):381-90. Epub 2010/09/28. doi:
721 10.1016/j.virol.2010.08.036. PubMed PMID: 20869739; PubMed Central PMCID:
722 PMCPMC2952651.
723

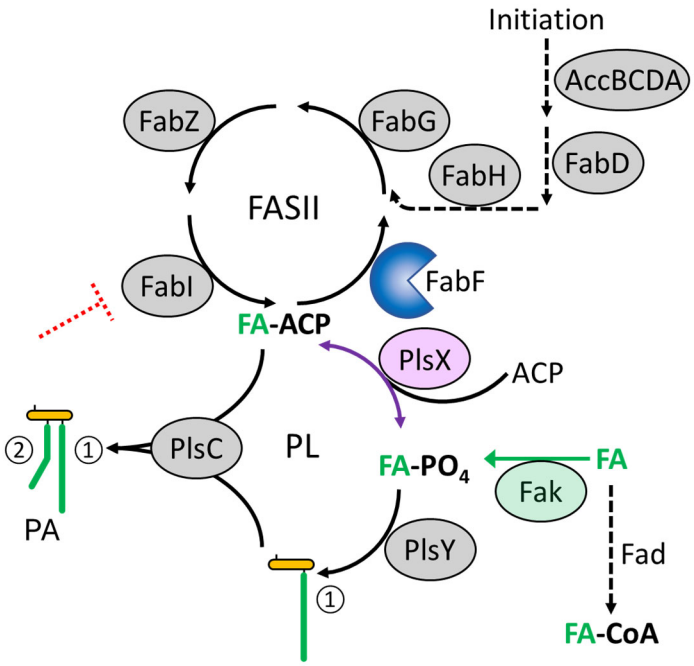

Fig. 1: Roles of the reversible PlsX enzyme in phospholipid synthesis. The FASII pathway schematized here produces acyl-ACP (FA-ACP), which may either be elongated by FASII using FabF (blue), or used by PlsX (purple) to initiate phospholipid (PL) synthesis. The PlsX product FA-PO_4 is a substrate for PlsY, a membrane protein that joins the acyl group to the glycerophosphate backbone in position 1 (①, bottom). PlsC then uses this intermediate product (lysophosphatidic acid), to add the second acyl moiety from FA-ACP to position 2 (②), generating phosphatidic acid (PA, left). Reverse PlsX activity uses phosphorylated exogenous FAs (green) produced by the FA kinase Fak [4], to produce FA-ACP. FASII inhibition (dashed red T) is bypassed by exogenous FAs [6], which are converted to FA-PO_4. The latter is used by PlsY to fill position 1, and by reverse PlsX, followed by PlsC, to fill position 2, thus producing PA. In a Δ*plsX* mutant, FAs charging position 1 are exogenous, while those charging position 2 are FASII-synthesized; in this case, the two FA sources are disconnected. See [1, 6, 9, 12] for references. Exogenous FA are subject to β-oxidation by FA degradation enzymes particularly in glucose-starved conditions (Fad, lower right; [25, 26, 50]). Enzymes circled in grey are not discussed in this study.

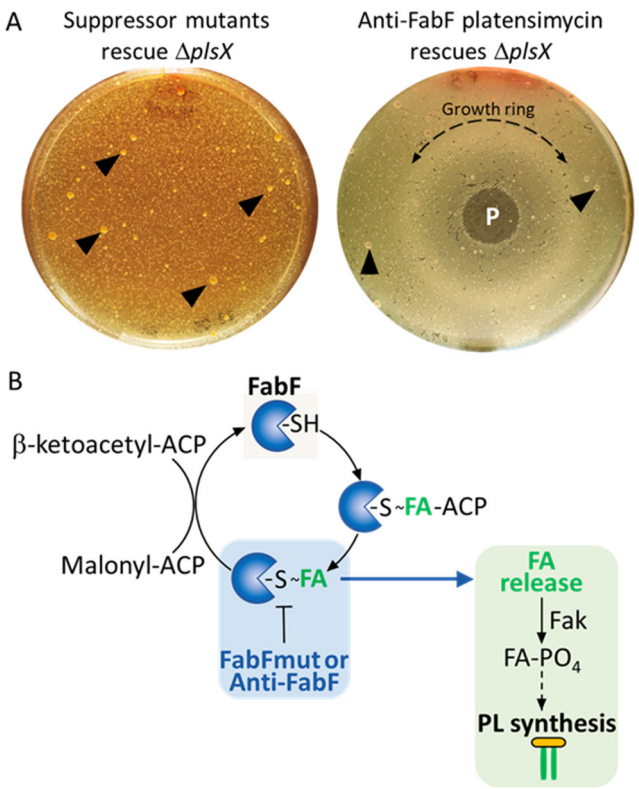

747
748
749
750
751
752
753 **Fig. 2. *fabF* mutants or the FabF inhibitor platensimycin rescues Δ*plsX* growth in the**
754 **absence of exogenous FAs. A.** Lawns of RN-R Δ*plsX* were spread on BHI medium without FA
755 addition, without (left) or with (right) 1.5 µg platensimycin (P) deposited in the center. Plates
756 were photographed after 4 days at 37°C. Black arrowheads, examples of suppressors, some
757 of which map to *fabF*. Dashed arrow (left), a homogenous growth ring surrounds the
758 platensimycin spot. N=4. **B.** Working model for Δ*plsX* growth rescue by a FabF mutation (FabF
759 mut) or by partial FabF inhibition by platensimycin (anti-FabF). FabF perturbations would
760 reduce enzyme processivity, such that the unstable FabF-FA intermediate releases FAs prior
761 to second substrate malonyl-ACP loading, as needed to bypass the Δ*plsX* defect. FabF in blue;
762 FAs in green. Symbols for FabF are based on [51].

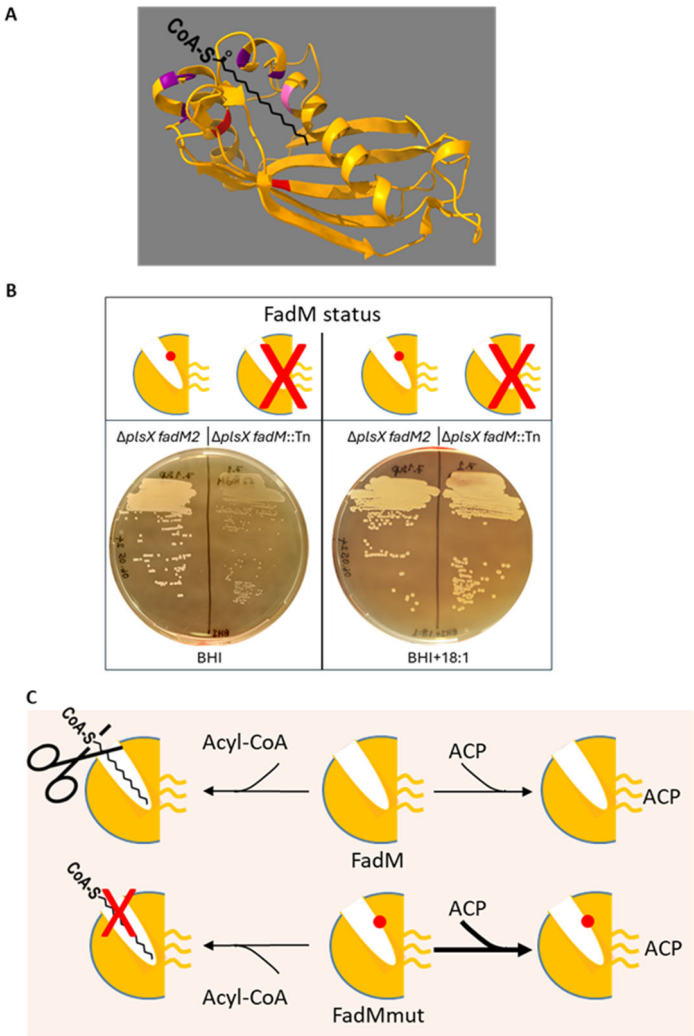

Fig. 3. FadM variants mapping to the predicted FA binding tunnel, but not FadM inactivation, confer the *fadM* suppressor phenotype. A. Schematized *S. aureus* FadM monomer binding to FA, based on crystal structure and Alphafold predictions ([20, 37], designed with https://alphafoldserver.com and http://www.cgl.ucsf.edu/chimera [52]). FA moiety (black line) binding in the FadM cavity involves amino acids Ile38 (pink), Tyr45; Met48, Leu122, Tyr125, and Phe126 (purple) [20]. The Δ*plsX* suppressors mapping to FadM affect amino acids Ile38Thr, Tyr90Phe, or Tyr133Phe (pink, and 2 red, respectively), which cluster around the FA-binding cavity; Ile38 (pink) is common to structural predictions and the FadM^{I38T} Δ*plsX* suppressor. **B.** FadM inactivation abolishes Δ*plsX* suppression: Growth of Δ*plsX fadM2* and the Δ*plsX fadM::*Tn derivative was compared on solid BHI medium without or with C18:1. Plates were photographed after 48 h growth at 37°C. Background growth on BHI (left) may be due to FA carryover from pre-cultures or to FA traces in medium. Plates are representative of biological triplicates. **C.** Working model for FadM *versus* FadM mutant function. Binding of the acyl-CoA FA moiety (zigzag line) in the FadM tunnel is needed for acyl-CoA thioesterase activity (scissor). FadM mutations in the tunnel (red dot) prevent this activity (red X) but conserve ACP binding (thick arrow, lower right).

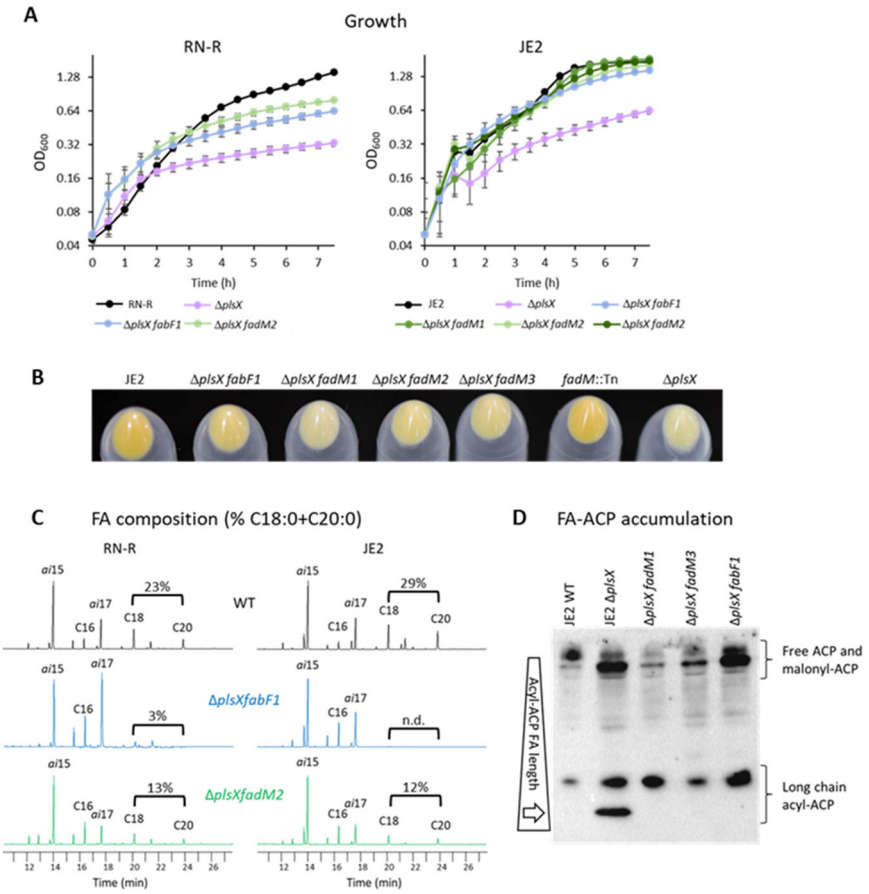

Fig. 4. Behavior of *fabF* and *fadM* suppressors of Δ*plsX* without exogenous FAs. A. Growth of WT *S. aureus* (RN-R or JE2), Δ*plsX*, and Δ*plsX fabF* or Δ*plsX fadM* suppressors in BHI medium**.** Left: RN-R WT, and derivatives: Δ*plsX*, and Δ*plsX* suppressors *fabF1* (encoding $FabF^{A119E}$) and *fadM2* (encoding $FadM^{Y90F}$). Right: JE2 WT, and derivatives: Δ*plsX*, and Δ*plsX* suppressors *fabF1*, *fadM1*, *fadM2*, and *fadM3* (encoding $FabF^{A119E}$, $FadM^{I38T}$, $FadM^{Y90F}$, and $FadM^{Y133F}$ respectively). Mean and standard deviation of independent triplicate cultures are shown. **B.** BHI + C18:1-grown overnight cultures of the indicated strains were pelleted, and photographed to compare pigmentation. C18:1 was added to include Δ*plsX* in comparisons. **C.** FA profiles of RN-R (left)- and JE2 (right)- derived WT, Δ*plsX*, and *fabF* or *fadM* suppressors determined from BHI-grown cultures. FA assignments are as indicated. *ai*, anteiso; even numbered FAs are saturated (e.g., C16 is C16:0). The main FA component of WT *S. aureus* is *ai*15 [7]. Peak heights correspond to relative responses (mV) of each FA in a sample. The proportions (in %) of C18:0 plus C20:0 of total FAs are indicated over the brackets. **Table S3** provides complete FA profile information. **D**. Acyl-ACP species in *S. aureus* JE2-derived Δ*plsX*, and Δ*plsX* suppressor strains. JE2 WT, Δ*plsX fadM1*, Δ*plsX fadM3*, and Δ*plsX fabF1* (isolates 7.5, 8.7, and 7.7, respectively; **Table S2**) were grown in BHI. The Δ*plsX* strain was pre-grown in BHI+C18:1 medium, and FA-starved for 2h in BHI prior to harvesting. Extracts were loaded on non-denaturing acrylamide gels, and immunoblotted using anti-ACP [7, 35, 53]. Longer FA moieties on acyl-ACP migrate faster on gels (wedge; [35, 54]). White arrow, accumulated acyl-ACP produced by FASII is not processed to phospholipids [5] (**Fig. 1**). Results are representative of biological duplicates.

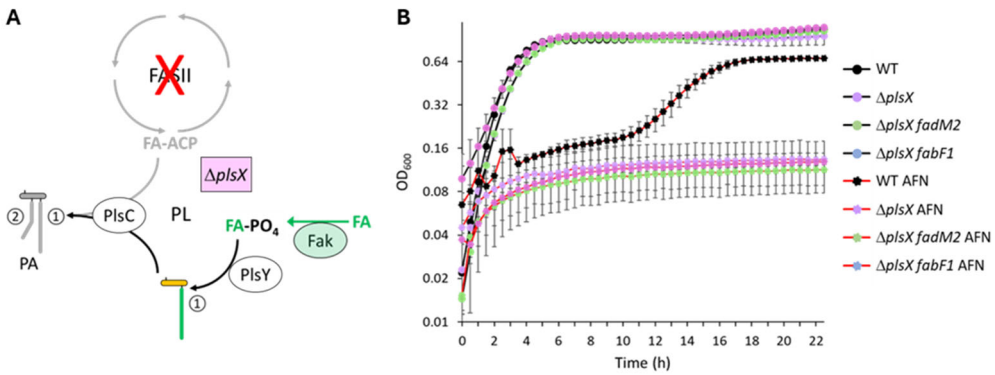

Fig. 5. Synthetic lethal effect of a combined FASII and PlsX block in Δ*plsX* and suppressor strains. A. Expected effects of FASII inhibition on an *S. aureus* Δ*plsX* mutant. In a WT strain, FASII inhibition by mutation or by antibiotic action is overcome by exogenous FAs, which are phosphorylated by Fak [4]. FA-PO_4 is the substrate for PlsY and for reverse PlsX activities, and is thus used for phospholipid (PL) synthesis at both the 1 and 2 positions. If both FASII and PlsX are blocked as shown, exogenous FAs can only fill position 1. The FASII defect or PlsX absence can be rescued separately by FA supplementation, but not the combination. Green, exogenous FAs and FA kinase; purple, *plsX* deletion; grey, pathways and products affected by combined FASII and PlsX block. **B.** Effects of anti-FASII treatment on JE2 Δ*plsX*, and Δ*plsX* suppressor strains in FA-supplemented medium. Strains were precultured in SerFA, and grown in SerFA without or with addition of 0.5 µg/ml anti-FASII AFN-1252. When the anti-FASII is added, WT *S. aureus* strains incorporate FAs to constitute membrane phospholipids, thus bypassing inhibition [6, 8, 55]. As Δ*plsX* suppressors cannot generate FA-ACP needed for FASII bypass [6, 9, 12], they remain sensitive to anti-FASII. Mean and standard deviation of independent triplicate cultures are shown. Black lines, no anti-FASII, red lines with anti-FASII. *fadM2* encodes $FadM^{Y90F}$; *fabF1* encodes $FabF^{A119E}$.

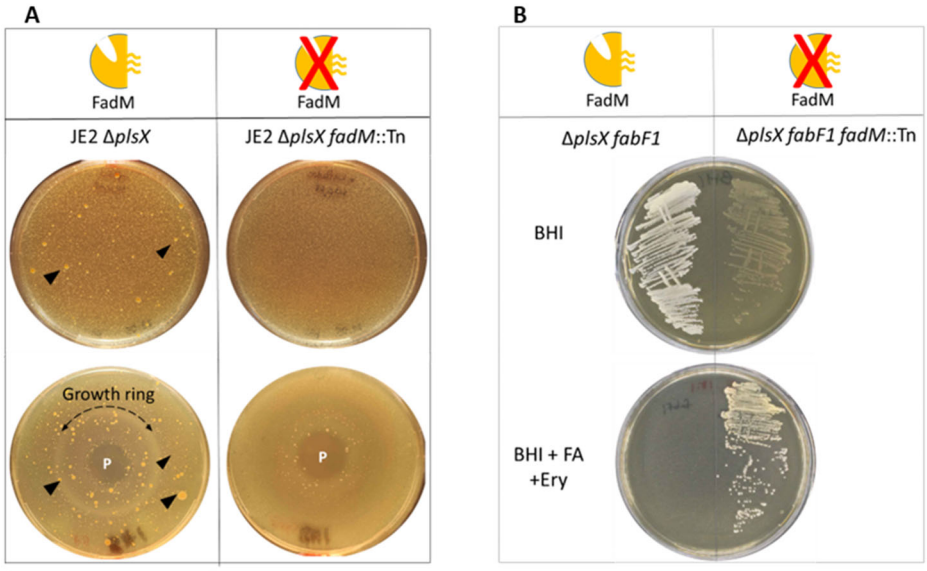

Fig. 6. *fabF* suppressors of Δ*plsX* require the presence of a *fadM* allele. A. FadM is present in JE2 Δ*plsX* (left) and absent in Δ*plsX fadM::*Tn (right, constructed from strain 7.1: **Table S2**). Strains were plated on BHI solid medium (100 µl of OD_{600} = 0.005), and in the lower set, spotted with platensimycin (P; 1.5 µg). Plates were photographed after 6 days at 37°C. Black arrowheads point to Δ*plsX* suppressor clones. The dashed curved line indicates the growth ring surrounding platensimycin spotting. The small colonies surrounding platensimycin on Δ*plsX fadM::*Tn lawns (right) failed to regrow on BHI medium. **B.** FadM is present in the JE2 Δ*plsX fabF1* suppressor strain (left) and absent in Δ*plsX fabF1 fadM::*Tn (right, constructed from strain 7.8: **Table S2**). Strains were streaked on BHI solid medium (upper), or BHI medium containing 250 µM C18:1 and 5 µg/ml erythromycin (Ery; lower). Plates were photographed after 24 h incubation at 37°C. Results are representative of three independent cultures and platings.

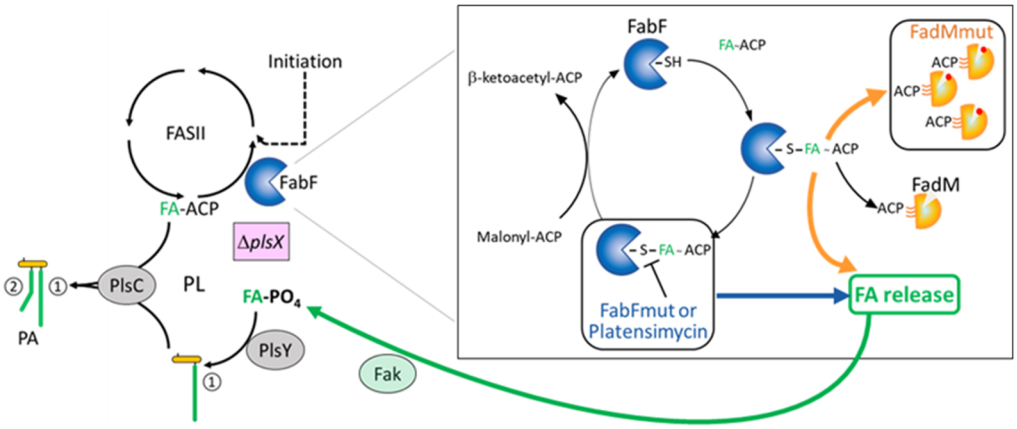

Fig. 7. Proposed role of FabF - FadM interactions in controlling FA release and recycling from FabF intermediates. Our study showed epistasis between FabF and FadM, and leads us to a working model of how these proteins interact (depicted in the inset). Left, FASII and phospholipid synthesis (PL) coupled pathways [1, 56]. The *plsX* deletion dissociates the pathways, such that exogenous FA is required for survival. Symbols are as in **Fig. 1**. **Inset:** FabF - FadM interactions coordinately overcome Δ*plsX* growth arrest when either function is mutated. In the first FASII step, FabF (blue packman and blue arrow) cleaves acyl-ACP (FA-ACP) to release ACP, which then allows malonyl-ACP entry into the FabF cavity to extend the acyl intermediate by 2 carbons [18, 38]. The FabF^{A119E} variant (FabFmut), or addition of anti-FabF inhibitor platensimycin, impedes malonyl-CoA entry, leading to FA release (FA symbols in green). FadM (gold) is bifunctional, with acyl-CoA thioesterase and ACP binding activities [20, 22-24]. Suppressor mutations in FadM (FadMmut red dot) alter the FadM acyl binding cavity, which we propose decreases acyl-CoA thioesterase activity as reported for FadM mutants also mapping to the binding cavity [20]. More FadMmut is thus available for ACP binding (boxed FadMmut). FadM-ACP or FadMmut-ACP binding could favor ACP release from the FabF pocket and leakage of FAs, which are then processed for PL synthesis *via* FA kinase (Fak) [4]. Symbols for FabF are based on [51].

886 **Supplementary Figures and Tables**

887

888

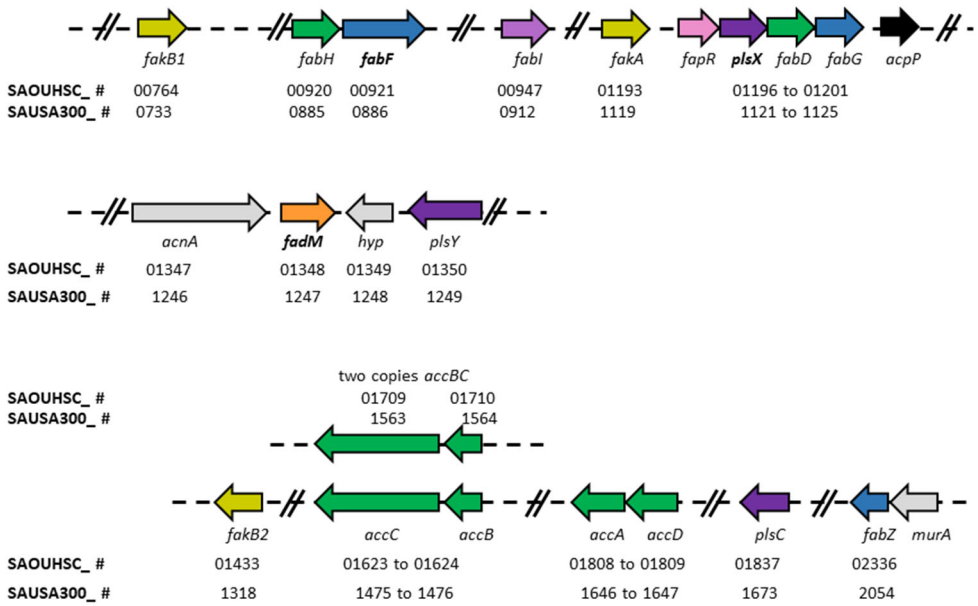

889

890

891

892

893

894

895

896

897

898 **Fig. S1. FASII and phospholipid gene organization in RN-R and JE2 strains.** Locus tags of
899 genes related to this study are presented. Dark green, FASII initiation; blue, FASII elongation;
900 black, acyl carrier protein (*acpP*); purple, phospholipid synthesis; olive, FASII bypass fatty acid
901 kinase; pink, regulatory; orange, FadM; grey, not directly related. Locus tags are given for
902 USA300 FPR_3797 8325-4 as references.

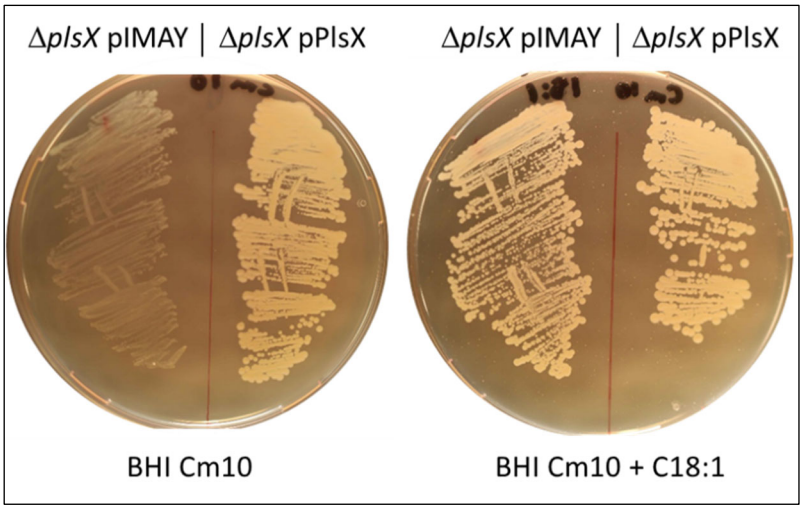

Fig. S2. Complementation of Δ*plsX* by a plasmid-carried *plsX* gene. RN-R Δ*plsX* strains containing an empty plasmid carrying a chloramphenicol resistance cassette (pIMAY; left side of plates), or a plasmid carrying the *plsX* gene expressed from its native promoter on pIMAY (pPlsX; right side of plates), were streaked on BHI-chloramphenicol (Cm) 10 µg/ml solid medium, without or with 250 µM C18:1 to bypass the Δ*plsX* defect. Background growth on BHI (left) may be due to FA carryover from pre-cultures or to FA traces in medium. Plates were photographed after 48h growth at 30°C. The Δ*plsX* strain carrying the empty plasmid failed to grow in the absence of C18:1 supplementation, while the pPlsX-complemented strain grew in both media.

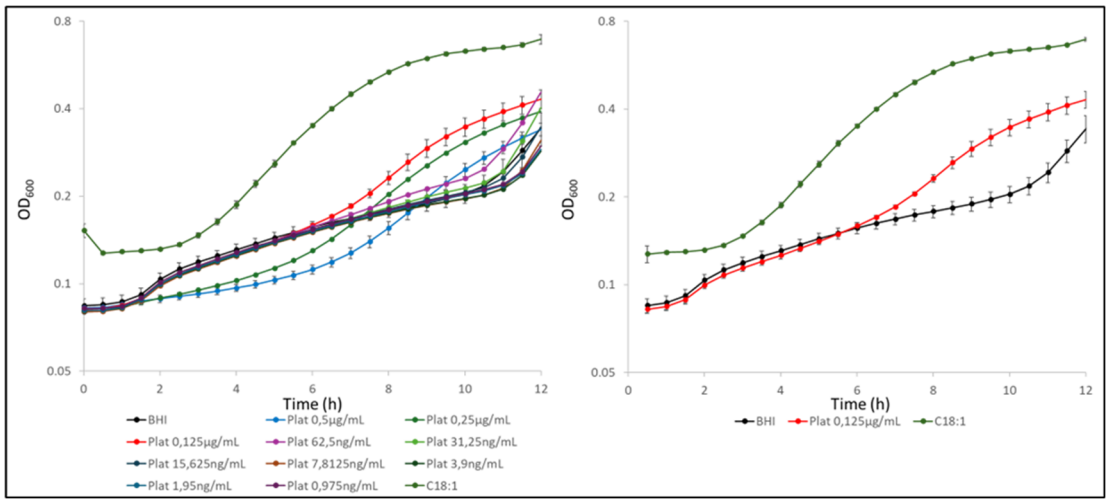

Fig. S3. JE2Δ*plsX* growth stimulation by platensimycin in liquid culture. JE2 Δ*plsX* was grown overnight in BHI medium containing C18:1. After washing, the strain was resuspended to OD_{600} = 0.05 and used to inoculate BHI medium to which platensimycin was added at the concentrations indicated below graphs. Left, growth curves with the different platensimycin concentrations added to medium. Right, the optimal concentration leading to improved growth with platensimycin (red line) compared to growth in BHI medium (black line). The averages of three independent triplicates are shown. Differences are statistically significant (P=≤0.05) by 2-tailed bilateral T-test for all points comparing Δ*plsX* growth in BHI and BHI plus platensimycin 0.125 µg/ml) between 7 h and 12 h growth.

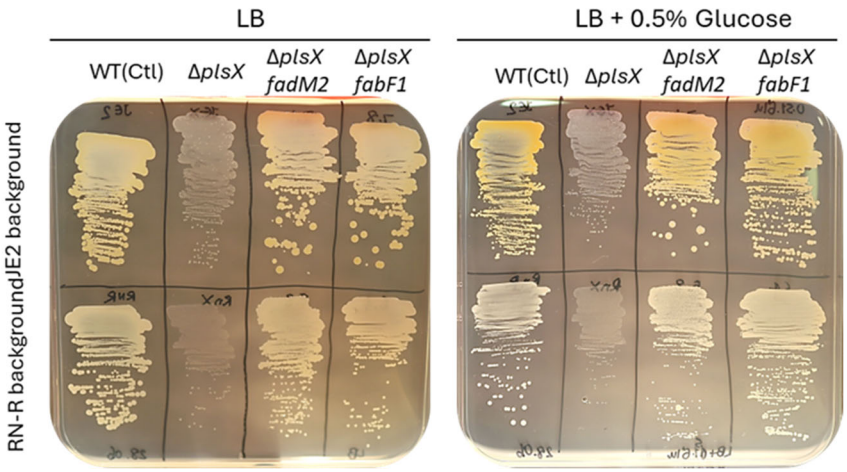

Fig. S4. FadM^m acyl-CoA thioesterase activity is not needed for Δ*plsX* suppression. A. The FadM^m suppressor phenotype is not subject to glucose repression, suggesting that the Fad-mediated acyl-CoA synthesis degradation pathway (Fad) is not involved. Fad enzyme FadE converts FA to acyl-CoA, a FadM substrate [20]. The *fad* operon is subject to CcpA-glucose repression [25-28], suggesting that acyl-CoA pools would drop in glucose-containing medium. Strains precultured in LB and LB with C18:1 for Δ*plsX* (Materials and Methods) were streaked directly on solid LB medium without or with 0.5% glucose. Background growth on LB (left) may be due to FA carryover from pre-cultures or FA traces in medium. Upper and lower rows, strains are derived from JE2 and from RN-R, respectively. Results represent biological triplicates.

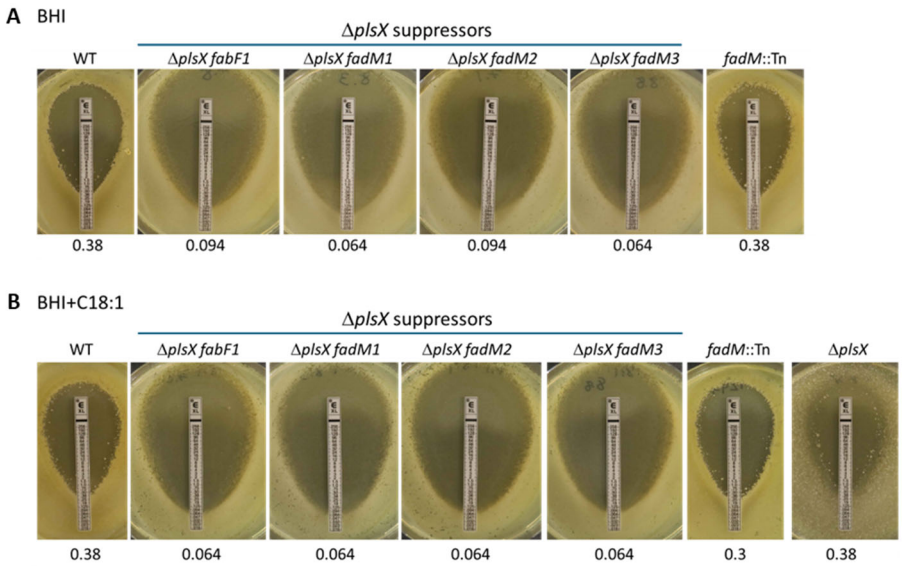

Fig. S5. MRSA JE2 Δ*plsX* suppressor mutants are sensitized to the β-lactam antibiotic amoxicillin. The indicated JE2 and Δ*plsX* derivative strains were grown overnight in BHI medium without (**A**) or with 250 µM C18:1 (**B**). Cultures were resuspended to OD_{600} = 0.1 and 100 µl were spread on the cognate solid media. Amoxicillin Etest strips were placed on plates, followed by 48 h incubation at 37°C. The amoxicillin MICs are indicated in micrograms per milliliter below each photo.

982

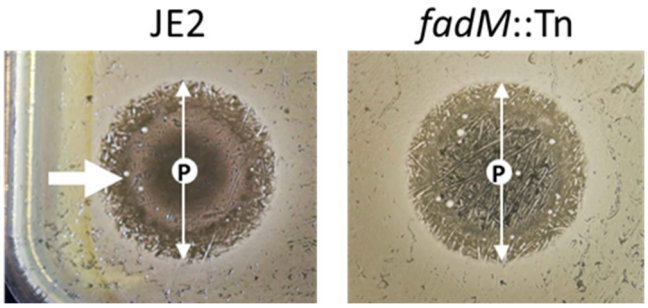

983
984
985
986
987
988
989
990
991
992
993 **Fig. S6. FadM is required for platensimycin-stimulated ring formation in the WT background.**
994 Overnight BHI cultures of JE2 and *fadM::*Tn (SAUSA300_1247) were washed in 0.9% NaCl, pellets were
995 resuspended to OD_{600} = 0.1, and 250 µl was spread on 120 x 120 mM square petri plates containing
996 solid BHI medium. Three µg platensimycin were spotted on plates ('P' in white circle; N=2). Plates were
997 photographed at 48 h. Vertical arrow, inhibition zone; left arrow, growth ring surrounds the
998 platensimycin deposit site in the WT, but not the *fadM::*Tn strain.

999 **Table S2. Δ*plsX* suppressors [a,b].**

	Gene : protein mutations in Δ*plsX* suppressor mutants				
	SAUSA300_0886 FabF (3-oxoacyl-ACP synthase II)		SAUSA300_1247 FadM (acyl-CoA thioesterase/ACP binding [20, 22-24])		
Strain name	*fabF1*: $FabF^{A119E}$	*fabF2*: $FabF^{D266A}$	*fadM1*: $FadM^{I38T}$	*fadM2*: $FadM^{Y90F}$	*fadM3*: $FadM^{Y133F}$
RN4220 5.1	X		NT	NT	NT
RN4220 5.2	X		NT	NT	NT
RN4220 5.3	X		NT	NT	NT
RN4220 5.4	X		NT	NT	NT
RN4220 5.5	X		NT	NT	NT
RN4220 5.6				X	
RN4220 5.7				**X**	
RN4220 5.8				X	
RN4220 6.1	X		NT	NT	NT
RN4220 6.2	X		NT	NT	NT
RN4220 6.3	X		NT	NT	NT
RN4220 6.4	X		NT	NT	NT
RN4220 6.5	X		NT	NT	NT
RN4220 6.6	X		NT	NT	NT
RN4220 6.7				X	
RN4220 6.8	X		NT	NT	NT
JE2 7.1				**X**	
JE2 7.2			X		
JE2 7.3				X	
JE2 7.4			X		
JE2 7.5			X		
JE2 7.7	X		NT	NT	NT
JE2 7.8	X		NT	NT	NT
JE2 8.1			X		
JE2 8.2				X	
JE2 8.3			X		
JE2 8.4			X		
JE2 8.5			X		
JE2 8.6			X		
JE2 8.7					X
JE2 8.8					X
JE2 Sup1 [b]	X				
JE2 Sup2 [b,c]		X			

1000

1001 [a] 'X' indicates that the mutation is present in the tested isolate. NT, not tested; without indication,
1002 no mutation detected by DNA sequencing. Suppressors identified from whole genome sequencing
1003 are in bold. [b] Sup1 and Sup2 suppressors of Δ*plsX* had the same secondary mutation in
1004 SAUSA300_100 (generating $Csa1A^{K185Q}$), which was absent in subsequently isolated suppressors
1005 mapping to *fabF*. [c] Sup2, encoding $FabF^{D266A}$, could not be propagated after storage.
1006 [b] Accompanying Excel Table S1. Sequence comparisons of Δ*plsX* suppressors and reference strains.

1007 **Table S4. Genetic materials.**

Strains			
Host strain	**Strain**	**Description**	**Reference**
JE2 USA300_FPR3757	JE2 (WT)	USA300_FPR3757 cured of its three native plasmids	[28]
	Δ*plsX*	In-frame *plsX* deletion leaving operon intact	This study
	Δ*plsX* suppressor in *fadM*; *ΔplsX fadM1*	*fadM1* encodes FadM^{I38T}	This study
	Δ*plsX* suppressor in *fadM; ΔplsX fadM2*	*fadM2* encodes FadM^{Y90F}	This study
	Δ*plsX* suppressor in *fadM; ΔplsX fadM3*	*fadM3* encodes FadM^{Y133F}	This study
	Δ*plsX* suppressor in *fabF; ΔplsX fabF1*	*fabF1* encodes FabF^{A119E}	This study
	fadM Tn insertion	JE2 derivative containing an erythromycin-resistance-marked transposon (Tn) insertion in SAUSA300_1247 at position 1384915 (based on JE2 genome entry NZ_CP020619)	[28]
	Δ*plsX fadM::*Tn	Φ80 phage transduction of the SAUSA300_1247 Tn insertional mutant into the Δ*plsX fadM2* (7.1, **Table S2**) suppressor	This study
RN-R 4220	RN-R 4220 (WT)	RN4220 derivative repaired for *fakB1*	[15]
	Δ*plsX*	In-frame deletion of *plsX* leaving operon intact	This study
	Δ*plsX* suppressor in *fadM; ΔplsX fadM2*	*fadM2* encodes FadM^{Y90F}	This study
	Δ*plsX* suppressor in *fabF; ΔplsX fabF1*	*fabF1* encodes FabF^{A119E}	This study
Plasmids			
	Plasmid	**Description**	**Reference**
	pMAD	Thermosensitive plasmid used to generate double-crossover deletion events	[42, 43]
	pMAD-*fapR-fabD* fragments	Used to generate *plsX* deletion	This study
	pIMAY	Used for *plsX* cloning	[44, 57]
	pIMAY-*plsX*	Used for *plsX* complementation in Δ*plsX*	This study
Transducing phage			
	Phage	**Description**	**Reference**
	ϕ80	Used to transduce erythromycin-resistance-marked Tn insertion of SAUSA300_1247 into Δ*plsX fadM2* and Δ*plsX fabF1* backgrounds	[58]

1008

1009

1010 **Table S5. Oligonucleotides (5' to 3') used for genetic constructions and mutant detection**.

Construction type and primers used for detection		Description
Plasmid for Δ*plsX* construction on pMAD linearized by SmaI		
pMAD_FapR_F	TCTATCGATGCATGCCATGGTACCCCTTCATCACAGACCATGAACTAAGC	*fapR* fragment
FapR_FabD_R	CGGAAAAATAATTGCTGTTTTACTCATAATTTTATCCTCGCTTATCATAAAAC	
FapR_FabD_F	GTTTTATGATAAGCGAGGATAAAATTATGAGTAAAACAGCAATTATTTTTCCG	*fabD* fragment
FabD_pMAD_R	GCAGAAGCTTCTAGAATTCGAGCTCCCTGTGACCTGAAACAACAATTTGACC	
Verifications for pMAD constructions		
pMAD_F	GTTACGTTACACATTAACTAGACAG	
pMAD_R	TGGACAGCATGGCCTGCAACGC	
Cloning *plsX* on pIMAY-derived locus1 plasmid		
pIMAY_FapR_F	AGTTTGTGGTTTAATGGGGTTGACACTTGAACTATTTAAA	*fapR* fragment
FapR_PlsX_R	TCAATTGCTAATTTAACCATTTTTTAGTACCTAGTCTTAA	
FapR_PlsX_F	TTAAGACTAGGTACTAAAAAATGGTTAAATTAGCAATTGA	*plsX* fragment
plsX_pIMAY_R	TTGTTGCTATAATGAAATGCGTTCTTACTCATTTGATTCACCTA	
pIMAY_FapR_R	TTTAAATAGTTCAAGTGTCAACCCCATTAAACCACAAACT	pIMAY linearized by reverse PCR
plsX_pIMAY_F	TAGGTGAATCAAATGAGTAAGAACGCATTTCATTATAGCAACAA	
Δ*plsX* suppressor verifications		
FabF_F	GGAATCAGCTAGAGAACGC	SAUSA300_0886
FabF_R	CATTTTTCAACCCACAAGAGG	
1247_F	AATCGGTATTTGAGGCAC	SAUSA300_1247
1247_R	ATCTTCACGCTAATTACATT	
0100_F	CGTGGCCTGGATATGATGAT	SAUSA300_0100 *csa1*
0100_R	GATTATCCTGAGCTACTTCG	
Verifications of Tn insertion in SAUSA300_1247		
1247_F2	GGATTACTATCGTCACGGTGG	Transposon insertion
UpBursa_F	CTCGATTCTATTAACAAGGG	
1247_R2	GTGTCCTGAACCTCGGAAGTTG	

1011